A laser-cut thermoformed orthosis for distal radius fractures

Revolutionizing fracture treatment

Tim van Helden

Rijnstate

UNIVERSITY OF TWENTE.

A laser-cut thermoformed orthosis for distal radius fractures

Revolutionizing fracture treatment

Author

T.M.N. van Helden, BSc. (Tim)
Technical Medicine | Medical Imaging & Intervention |University of Twente | Enschede

Graduation committee

Chairman

Prof dr. ir. K. Slump (Kees)
Faculty of Electrical Engineering, Mathematics and Computer Science (EEMCS) | University of Twente | Enschede

Medical supervisor

Dr. E. Hekma (Edo)
Trauma surgery, Lung surgery| Rijnstate hospital | Arnhem

Technical supervisor:

Ir. E.E.G. Hekman (Edsko)
Faculty of Engineering Technology (ET) | University of Twente | Enschede

Process supervisor:

Dr. M. Groenier (Marleen)
Faculty of Science and Technology (ET) | University of Twente | Enschede

External member:

M. van Helvert, MSc (Majorie)
Multi-Modality Medical Imaging (M3I) | University of Twente | Enschede

Colloquium

Date	September 29th 2020
Time	2 PM
Place	Online

PREFACE

Back in 2013, I did not know whether Technical Medicine would be the right education for me. However, after 6 years I found out that I could not have chosen better. I love to do research that can be implemented almost directly. Project groups taught me how to tackle problems from different points of view and physical practicums are a pleasant alternation to the literature research.

In my 3-month internship at the Rijnstate hospital, I loved the atmosphere of the department and being able to bring in new ideas and execute them. I purposely avoided certain aspects of the orthosis in this internship because I thought they would not fit in a 3 month schedule. However, when I got to choose my graduation internship I wanted to go back to Rijnstate to speed up the progress and tackle the challenges that followed. At the end of September 2019, I started my graduation internship at the Rijnstate hospital and mostly independently solved them. The people around me provided a pleasant environment with whom I could relieve some tension and they would ask me the right questions to help me continue with the project. It was unfortunate that the Corona crisis happened at the halfway point of my thesis and I certainly missed all the interactions that were limited because of it. It did make me realise even more how personal interactions stimulate my thoughts.

I would like to thank the following people for contributing to my report. In the Rijnstate hospital, I had many colleagues that provided me with positive energy and with whom I worked together. Edo always excited me to continue to work on the project and gave me lots of opportunities to grow in clinical practice. Edsko made sure my report was scientifically accurate and helped in the thought processes that led to innovative solutions while prof. Slump helped me to look at my reports from a different perspective. I hope you will enjoy reading this thesis as I am sure proud of what I have developed.

Tim van Helden

Arnhem, 17-9-2020

ABSTRACT

Background - Distal radius fractures are the most common type of orthopaedic fractures. Treatment is usually performed by immobilizing the wrist in a plaster cast for 3-5 weeks. However, these casts suffer from poor ventilation and do not always fit properly which can result in complications such as cutaneous diseases, bone and joint injuries or malunion. Therefore a movement towards 3D printed personalised orthoses has started as an alternative to tackle these problems. These orthoses can tackle the aforementioned problems, however, long manufacture times slow down or restrict implementation. Consequently, in this thesis, the goal was to develop a method to quickly manufacture an orthosis for distal radius fractures. But to test the method, an algorithm had to be developed because no open-source algorithms were able to produce a (2D) orthosis directly.

Design – The approach of this thesis was to increase speed by producing the orthosis flat instead of in 3D. A thermoformable material was chosen for increased rigidity and to avoid complicated cuts in the design which excluded several printing techniques. After evaluation, laser cutting was expected to speed up the production process the most and would be the most cost-effective. Both the EinscanPro and occipital scanner were used to scan the wrists. The orthosis was designed in Rhino 6 with Grasshopper. Both a Voronoi and Hexagonal pattern were investigated.

Development – Due to the organic properties of the wrist, the Voronoi pattern produced a better fitting pattern than the hexagonal pattern, especially at the corners. Thus, after a few prototypes, only the Voronoi pattern was continued. At first, the planning was to use a finite element model to optimize and test the stiffness, but due to the large mesh-reduction necessary to perform stress calculations with Fusion 360, real-life tests were performed instead as performed in Nieuwenhof 2020.

Validation – The results of the stiffness validation test and the theoretic comparison of the stiffness showed that the built orthosis is less stiff than a normal plaster cast. The comfort for short wearing times was adequate except for the thumb.

Conclusion – The algorithm that is developed is capable of producing a 2D or 3D design that can be either printed or laser-cut. The combination of designing flat and laser cutting can produce an orthosis significantly faster than 3D printing. Further testing and improvement of the wear comfort are necessary to start a pilot study with patients.

LIST OF ABBREVIATIONS

DRF	Distal radius fracture
FDM	Fused deposition modelling
FFF	Fused Filament Fabrication
PLA	Poly Lactic Acid
ABS	Acrylonitrile butadiene styrene
3D	three-dimensional
SLA	Stereo Lithography
DLP	Digital Light Processing
CFF	Composite Filament Fabrication
SLS	Selective laser sintering
STL	Surface Tessellation Language
BREP	Boundary representation

TABLE OF CONTENTS

0. INTRODUCTION

Distal radius fractures (DRFs) are the most common type of orthopaedic fracture accounting for around 25% of fractures in the paediatric population and up to 18% of all fractures in the elderly age group.[1,2] DRFs are conventionally immobilized with a plaster cast for 3 weeks for stable fractures and 4-5 weeks for unstable fractures. However, these casts suffer from poor ventilation and do not always fit properly which can result in complications such as cutaneous diseases, bone and joint injuries or a nerve palsy.[3–5] Other disadvantages are the high weight and the fact that the cast is unhygienic because it is not waterproof and thus cannot be cleaned.

To resolve these problems, several companies have come up with designs that use 3D printed casts as an alternative to the conventional plaster cast.[6–9] They use stronger materials, a more open design and use a 3D scanner to measure the upper limb to produce a personalised orthosis. In a typical 3D print workflow, first, a conventional plaster cast is placed and after 6 days the plaster cast is replaced with a fibreglass cast. Then, when the swelling is down, a 3D scan is made directly, or 2 or 3 days later if the wrist is still swollen. After the scan, the conventional cast is put back on for the 2 days in which the orthosis is produced. And after that, the orthosis is finally placed around the arm. This process is cumbersome and adds a few additional steps and costs compared to the conventional cast treatment.

Moreover, only a few of the designs have been clinically implemented. Currently, a few are used in local centres in the USA, Latvia, Brazil and Spain.[10] The main challenges that they face are the long printing time and the unpredictability of the swelling. The slow printing speed is partly being solved by using faster resin-based printing, but this technique uses resins that are toxic pre-curing and produce toxic waste as well. The problem with swelling is that it can change the shape and diameter of the wrist drastically within a few days. Also, wrist-casts have to be worn for 3-6 weeks with a trend of shorter immobilization.[11] This means that the benefits of an orthosis may only be applicable for half of the wearing time of the cast. To fix this issue, the swelling should be estimated beforehand and the orthosis should be adjustable so it can be worn from the start.

A 3D printing lab in Milan, called PiuLab, has a design available that uses flat printing and thermoforming to produce home-made orthoses. The orthosis is printed with a thermoformable material, heated in an 80-degree Celsius bath and folded around the wrist while cooling. Printing on a flat surface reduces the amount of needed support material which allows for faster printing and cuts down cost. Thermoformable plastics have the additional benefit of being able to be remodelled after the swelling is reduced, thus the same material can potentially be re-used and the orthosis directly worn from the start. It should be noted, however, that a company with a similar design still initiates treatment by applying a conventional cast. Only after 7 days, the cast is replaced by the orthosis. This may be explained by the fact that they state that the PLA can be formed 4 times after heating before shape-memory is acquired which may become an issue when remodelling the orthosis after 6 days[12]. However, another company that uses a similar technique uses a coating that ensures that the material they use can be remodelled indefinitely until the coating is removed.[13]

Most orthosis-manufacturers use a Voronoi pattern in their designs. A few use a hexagonal pattern with extra support. Silva 1997[14] et al and Angelucci et al. 2018[15] found that the strength of a random generated

Voronoi pattern is reduced by 30% compared to the regular hexagonal pattern. This is because individual cell walls endure higher strains compared to a regular pattern. However, the Voronoi pattern also increases the stiffness of the orthosis by a varying amount depending on the density.[14–16] Also, it is crucial that the fracture is unable to move during treatment and thus it may be more beneficial to trade strength for increased stiffness. Furthermore, since the strength and stiffness required for the orthosis is not uniform in every direction, a pattern that is adjusted to the wrist-dependent applied loads can reduce the total weight of the orthosis.

In this thesis, the goal is to combine the benefits and advances that are made with the 3D printed casts that are used after 10 days with the low-cost and fast-manufacturing speed of thermoformable plastics. This includes a force optimised structure, tailor-made for the location and type of fracture, and the ability to produce the orthosis flat, which excludes the need for support material and reduces costs. Additionally, the size measurement technique of the wrist will be improved. Moreover, the orthosis has the potential to be remodelled after the swelling is reduced, which is an important property of the material to be more cost-effective. To acquire an orthosis with sufficient strength and rigidity, the necessary strength to immobilize the fracture will be investigated The end goal will be a design that is ready to be used in clinical trials and has been tested on volunteers. Since no publicly available algorithms exist that combines all these features, an algorithm will be developed to test the possibilities of the thermoformed orthoses. The design will have improved ventilation, reduced pressure points, a tight fit and can be implemented from the start of immobilization.

The thesis is structured as follows: first, in the medical background (chapter 1) physiological processes that occur during a fracture are explained together with treatment options. Next, in the technical background (chapter 2) the concept of producing an orthosis flat is introduced followed by the printing techniques. Then, in chapter 3 the solution requirements are formulated. In chapter 4 and 5 the design and development of the orthosis are explained. Finally, in the last chapters, the results are discussed and some future recommendations are proposed.

1. MEDICAL BACKGROUND

In this chapter, basic knowledge of the medical terms that are used in this thesis is explained. Next, the most important anatomical structures for DRF treatment are pointed out. Subsequently, the types of fractures that can be differentiated will be covered and lastly, the treatment options are discussed.

1.1 Anatomical structures and medical terms

The lower arm consists of 2 bones: the Radius and the Ulna. With a DRF, the distal side of the radius is fractured. A DRF is also called a wrist fracture since the fracture is close to the wrist joint or the wrist is involved. The ulnar styloid process and radial styloid process are bulges of the ulna and radius respectively, which often cause pressure points while wearing a cast because of its protrusion compared to the wrist (Figure 1.1). Occasionally, nerve palsy occurs in the ulnar- or radial nerve due to a tight cast. The anatomical positions are shown in figure 1.1B.

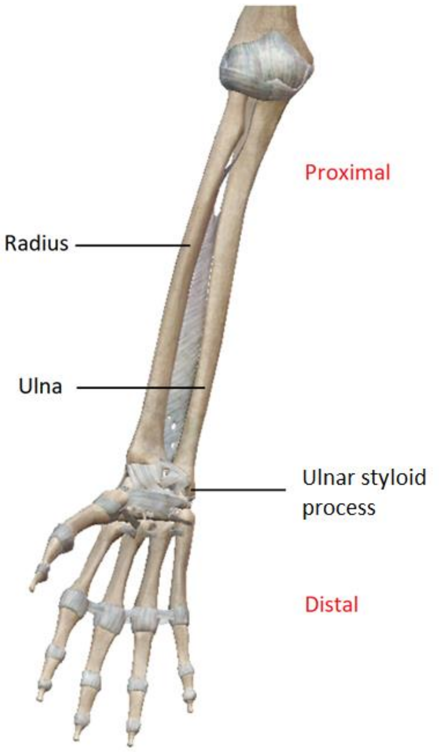

(A)

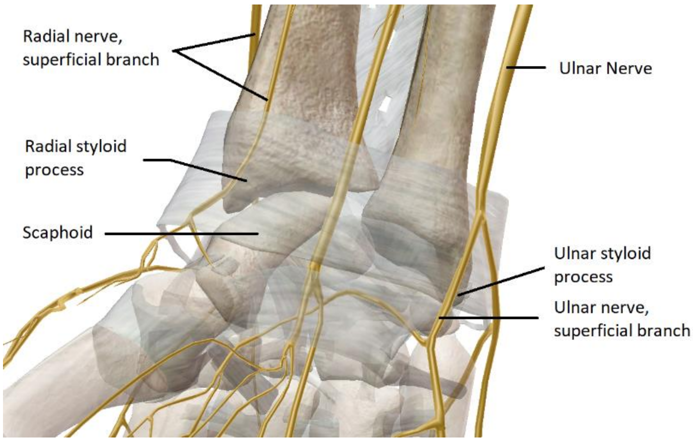

(B)

Figure 1.1 Anatomical landmarks of the upper limb

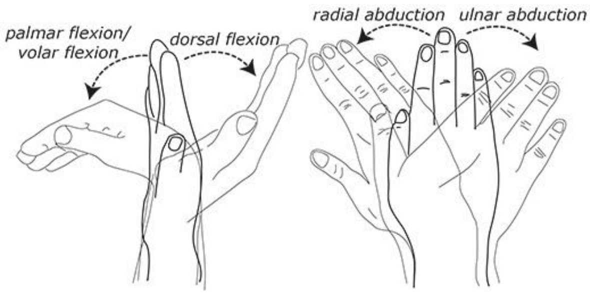

Figure 1.2 Anatomical directions of the wrist

As shown in figure 1.2, (Palmar) flexion is the movement around the wrist in the direction of the palm of the hand while dorsiflexion or extension is movement in the opposite direction. Secondly, radial abduction and ulnar abduction is the movement of the hand with the wrist joint towards the radius or ulna respectively.

1.2 Stability of the fracture

Depending on the stability of the fracture as observed on a radiographic image, a treatment plan is made. The fracture is classified as either stable or unstable depending on a few definitions. The first and most common definition for an unstable fracture is that the fracture does not hold its position after closed reduction. The second definition is of Lafontaine et al [17] which states that if 3 or more of the following definitions are met, the fracture is unstable: dorsal angulation exceeding 20°, dorsal comminution, intra-articular radiocarpal fracture, associated ulnar fracture and age over 60 years. The third most common definition states that the fracture is unstable when it is a volarly displaced fracture such as Smith's or reversed Barton's fracture.[18] The different types of fractures are explained below.

1.3 Types of fractures

For all fractures, first, a radiographic image is taken in the anterior-posterior and lateral direction. For complicated fractures that may need surgery, a CT scan is made for better decision making. After an assessment, distal radius fractures are classified into four groups. First of all, the most common type called Colles' fracture is usually caused by a fall forward with an outstretched hand and causes the radius to fracture extra-articular in the dorsal direction. Colles' fractures are frequently stable, thus hold their anatomical position after reposition. The properties of the fracture allow for more flexion than extension of the wrist without shifting the bones out of position. Secondly, the Smith's fracture is caused by falling onto flexed wrists and is an extra-articular fracture with the radius moved in the volar direction. These fractures are often unstable and need surgery to keep the radius and fragments into position. Next is the Barton's fracture, this is an intra-articular fracture and can be both in dorsal and volar directions with the latter called a reverse Barton's fracture. This fracture always needs surgery unless the fractured bone fragment is too small to be fixated onto the radius. The last type of fracture is the Chauffeur's fracture (figure 1.3d) and is caused by a force of the scaphoid onto the radial styloid process which causes avulsion of the radial styloid.


(a)

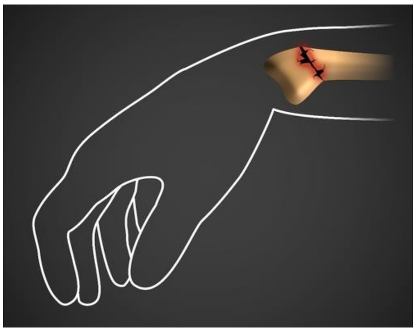
(b)

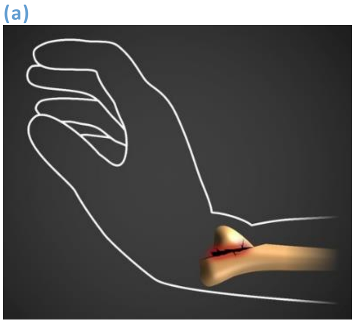
(c)

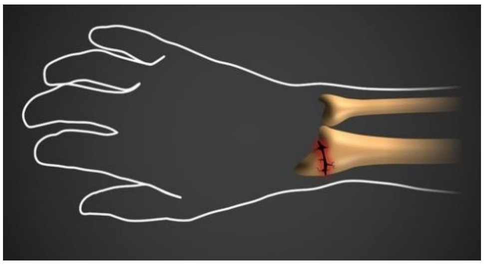
(d)

Figure 1.3: (a) Colles' fracture, (b) Smith's fracture, (c) Barton's fracture, (d) Chauffeur's fracture

1.4 Swelling

After a fracture occurs, the blood vessels inside the bones and surrounding tissue are damaged which causes swelling and bruising also known as fracture haematoma. This causes a chain reaction of inflammation, repair and remodelling. Depending on the fracture, primary cortical bone healing or indirect, secondary bone healing occurs. Direct bone healing occurs only with open reduction and internal fixation because the bone needs to be aligned correctly with a maximum gap of 0.01mm for contact healing and 1mm for gap healing. That is why usually only secondary bone healing takes place which causes swelling and callus forming, which do not occur with primary healing, partly because the fracture haematoma is removed during surgery.[19]

With secondary bone healing, the damaged tissue releases cytokines which start up the healing process involving immune cells and molecular factors. Polymorphonuclear neutrophils (PMNs) are the first cells to accumulate at the fracture site which then send out cytokines to attract macrophages, endothelial cells and fibroblasts. Endothelial cells form new blood vessels. Next fibroblasts are producing new collagen and stimulate crosslinking in the hematoma which results in the hematoma being replaced by a scaffold of granulation tissue with collagen fibres, cells and invading capillaries. Then macrophages activate the systemic process of replacing cartilage with bone by osteoblasts.[20] After 3 months around 70% of the fracture will be repaired and an end phase can be expected after 1,5-3 years while remodelling can continue up to 5 years according to Wolff's law[21]. The predictability of the swelling that occurs in the process of inflammation, repair and remodelling is quite difficult, which is a challenge when fitting an orthosis.

1.5 Treatment

Repositioning of the radius can be performed open or closed. Closed reduction is the preferred option and is performed with intact skin without performing surgery. But when repositioning is not possible with a closed skin, e.g. with an unstable fracture or when bone fragments and debris have to be removed, open repositioning is performed. During open-repositioning, the skin is opened surgically to reposition the bone fragments. Often a fixed metal (volar) plate is then placed with screws to stabilize the bones in their anatomical position. With a closed reduction, the protocol is that a plaster cast is always placed on the wrist to relieve pain and to hold the anatomical position of the bones for 3-5 weeks. However, some papers argue that after only 1 week, the function of plaster casts for stable non-displaced fractures is mostly pain relief. For reduced fractures, the stabilisation period has to be longer.[11,22] The need for a plaster cast after open reduction has to be assessed per patient because the metal fixation plate is usually able to stabilize the fracture without the need of a plaster cast. Nevertheless, before surgery, a plaster cast is often placed to bridge the time between the accident and surgery.

1.6 Muscles and muscle loss

Muscle loss is a common problem that occurs during the healing process of a fracture. The average amount of strength and muscle loss after 3-4 weeks is 14% and 4%, respectively.[23] Because the fracture has to be fixated, certain muscle groups are inevitably restricted in their movement. However, with a plaster cast, all muscles in the wrist joint are restricted, but this may not have to be necessary. It is known that certain movements of the joint could be allowed with certain fractures and under controlled conditions. For a Colles' fracture flexion of the wrist would be permissible. If an orthosis could allow flexion of the wrist but prohibit extension, this could decrease muscle loss of the flexors in the upper limb.

2 TECHNICAL BACKGROUND

In this chapter, first, the concept of producing the orthosis flat is introduced. Then the different 3D scanners are introduced. Next, the design formats that are used for representing 3D structures in the virtual space are illustrated. Finally, different ways of producing an orthosis are described to understand the benefits and limitations of each technology.

2.1 Folding the orthosis

One of the most important problems to date is the speed of 3D printing orthosis. A normal 3D FDM printer takes between 3-9 hours to print an orthosis depending on size and complexity. In clinical practice, this causes both an inappropriate amount of strain on patients and the maximum capacity of the hospital would quickly be reached for acute fracture treatment.

The most common way to produce an orthosis is to use 3D printing to directly produce the orthosis in its final form. However, an alternative is to produce the orthosis flat and use thermoforming to fold it around the wrist which could speed up production. When a scan is made and a mesh is produced, the surface of this mesh should be equivalent to the surface of the skin on which the orthosis has to be formed. This shape looks similar to an hourglass. Then the surface is virtually unfolded to a 2D shape and is produced flat. During application, the flat orthosis is heated in e.g. an 80 °C water bath, dried with a towel and moulded around the wrist. During curing the shape can be tweaked to be formed exactly to the shape of the wrist.

2.2 3D Scanners

Wrists can be measured by a tape measure, but to truly produce a personalised orthosis, many circumferential diameters are necessary. To obtain the entire shape of the wrist, 3D scanners use infrared or structured light to convert a real-life object into the virtual space. The technology has gained speed and precision and has lowered in costs over the past few years, thus has become available for more applications. The hand-held scanners both use structured light that is emitted by a projector in a non-uniform pattern and recollected after it has reflected off an object. The intensity and distortion of the reflected light are compared with the internal (calibrated) reference pattern and provides an estimation of the shape of the object and the distance between the camera and the object.[24] The Occipital structure scanner uses infrared light, whilst the Einscan Pro uses white light. However, blue light is becoming the new standard because of its higher accuracy and because it can be better corrected for reflections and transparency. With these hand-held scanners, a 360-degree walk-around is necessary to obtain a 3D image of an object in which the arm could have moved. A scanner that tackles these problems is manufactured by a Dutch company called Manometric, which uses a circular optical scanning tunnel with 360-degree vision. With this scanner, the patients only have to hold their hand stationary for 0.1 seconds and operator variability is non-existent. This device, unfortunately, is not (commercially) available yet in the period of this thesis.

2.3 3D design formats

The most common type of 3D print saving formats is the Surface Tessellation Language (STL) file. This format is based on polygon meshes. Polygon meshes are represented by vertices, edges and faces as shown in figure 2.1. Vertices represent the position of points in 3D space along with the colour, normal vector and texture coordinates. Edges consist of the connection between 2 vertices, while faces are a closed set of edges and can either be triangular- or quad faces. Most printers can only handle this format. However, this format uses vertices that are combined with triangles and thus do not give a very smooth and accurate representation of curving surfaces nor does it allow for easy manipulations. In contrast, surfaces can be easily manipulated with software programs such as Rhino 6, but polysurfaces (objects that consist of multiple surfaces) cannot. This will be important later during the development of the algorithm.

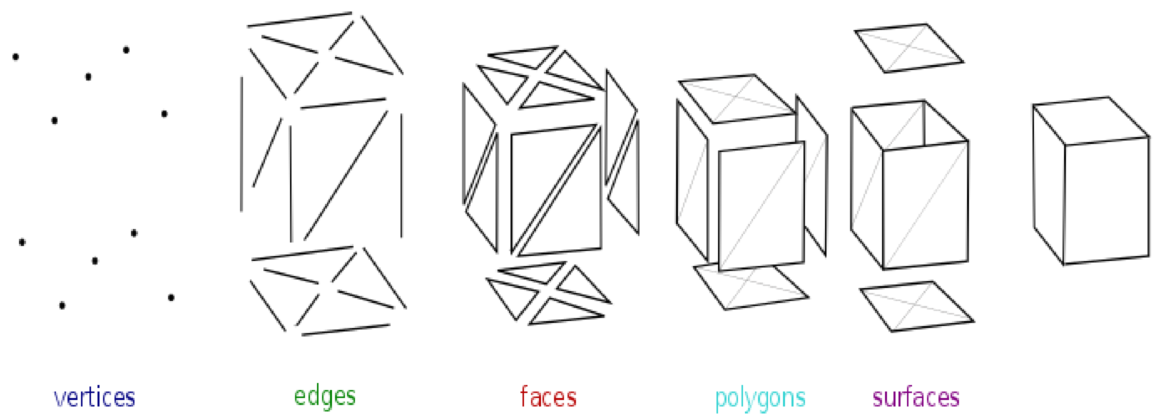

Figure 2.1 Elements of polygon meshes - reprinted from Wikipedia/Polygon_mesh

Another way of representing objects is by using a non-uniform rational basis spline (NURBS). This format is well supported by design-, manufacturer- and engineering software which enables e.g. strength calculations and optimization algorithms. Its shape represents a curve that is based on control points.

2.4 Production techniques

The techniques that are suited for the producing of orthoses are explained, thus the techniques only suitable for metals and ceramics are not mentioned since these materials are heavy and uncomfortable on the skin.

2.4.1 MATERIAL EXTRUSION

Fused deposition modelling (FDM) or also called Fused Filament Fabrication (FFF) is the most common printing technique worldwide. It is the least expensive option and is easy to use because the equipment itself is easy to maintain. However, for a smooth end-result, post-production steps are necessary to obtain a smooth finish.

FDM uses a heated extrusion nozzle to extract plastic filament onto the heated print bed. FDM can be used to print thermoplastics such as Poly Lactic Acid (PLA) and Acrylonitrile butadiene styrene (ABS). The product is formed layer by layer and the layer thickness and printing speed are determined by the size of the printing nozzle. A larger nozzle increases printing speed but decreases the accuracy of the parts. Composite Filament Fabrication (CFF) uses an extra printing nozzle that continuously lays down a composite filament. This technique increases the strength of the material in the direction of the fibres.

2.4.2 PHOTOPOLYMERISATION

Photo polymerisation uses a liquid Resin and light to cure the product. The 2 common curing-process types are stereolithography (SLA) and Digital Light Processing (DLP). SLA uses a laser, while DLP uses a projector to form very thin layers of plastic. SLA uses a galvanometer to send light rays to exact coordinates on a mirror below the resin which deflects the rays to the surface of the lifting plateau where they cure the product bottom-up. Unlike SLA, DLP uses an LCD screen-type beamer to cure all points in one layer simultaneously which can increase speed but limits the building size or accuracy and the LCD pixels cause a voxel pattern in the end product. Both techniques have very high accuracy and produce products with a smooth finish without post-processing. However compared to FDM, cleaning and maintaining the equipment is more involved and after printing, the material often has to be UV-cured.

2.4.3 POWDER BED FUSION

Powder bed fusion is a technique that uses either a laser or an electron beam as a heat source to melt material powder together as a product. For plastics, the most common technique is Selective laser sintering (SLS). SLS uses a laser and a powder roller to create the product layer by layer. For each layer, the whole build platform has to be full of powder (the powder bed) and post-production the powder is re-used. The build platform is lowered every single layer. Printing per layer is especially efficient when objects are flat.

2.4.4 LASER CUTTING

Laser cutting is different from the other techniques as it does not build the product up, but rather only cuts an existing sheet of material. The most common type of laser is the CO2 laser with a power of 100 or 150 Watt. The laser tube is situated on the back of de device and is reflected towards the cutting-surface via 3 mirrors that can position the laser over the cutting bed. Usually, a laser with a fundamental wavelength of 10.6 microns is used because it is most suitable for cutting plastics and other common materials.

3 SOLUTION REQUIREMENTS

In this chapter, the most important design requirements for the orthosis are summarised. Each requirement will be taken into account for in the production of the orthosis. The list starts with the most important requirements and ends with the least important.

Stabilizes the fracture

The most important task of the orthosis for displaced fractures is to stabilize the fracture in an anatomical position to promote a functional healing process.

Pain relief

The second most important task of the orthosis is to relieve pain caused by movement of the fracture. The fracture can be anatomically stable but still cause pain due to small shear movements. For stable fractures, pain relief is the most important feature after 1-3 weeks of wearing the orthosis depending on individual differences.

Fit

One of the problems with current plaster casts is that they cause pressure points at protruding locations of the wrist (mostly the processes ulnae). Also with new 3D printed orthosis fitting problems occur over time due to reduced swelling and muscle atrophy. The orthosis should be personalised as much as possible based on anatomy and injury type to prevent such fitting problems. The orthosis preferably is adjustable depending on swelling.

Adequate ventilation

Ventilation is important for skin-quality, hygiene, water evaporation and wearing comfort. Skin-quality will remain intact when exposed to the elements and when it can 'breathe'. With proper ventilation hygiene will improve because the skin does not become soft, smells do not build up under a layer of fabric and because less odour will be caused by sweat.

Waterproof

If the orthosis would be allowed to become wet, this would have many benefits. Firstly hygiene would improve significantly since the orthosis can be washed. Secondly, it would be convenient if no dry-bags would have to be used during showering, and swimming would become possible which improves physical function.[25]

Skin-friendly

The orthosis should not cause a rash, should be smooth such that is does not scrub the skin. It also should not smell, cause allergies or be toxic (when producing).

Affordable

The current plaster cast treatment is low-cost. The materials cost are €6,25-12,50 per cast, depending on the number of rolls used. No expensive (printing) devices are necessary. Including the cast technician, total conventional costs are estimated to be €70 according to ten Brinke 2019[26]. Since the treatment is applied approximately 25 times per day in the Rijnstate hospital alone, decreasing this cost would come with many benefits. A reasonable amount of cost is estimated to be up to €100,-.

Short production and application time

Conventional casts are quickly put on and traumatic patients can be treated very quickly. The patient should not have to wait long and have an effortless experience. Production should be on the spot and should not exceed 45 minutes.

Locking mechanism

The locking mechanism is an important part of the orthosis of which opinions differ per practitioner on what the design should look like. The common consensus is that it is desirable that the fit can be adjusted depending on swelling and muscle atrophy. Whether the patient should be allowed to do this themselves in the first week after the fracture is a matter of discussion between medical doctors since therapy compliance is a factor to take into account.

Visibility and radiology

The state of the fracture and the skin should preferably be well visible, both under an X-ray photo and by visual inspection. Conventional casts do not allow visual inspection and only the plastic reinforced cast allows for good vision during an X-ray photo. 3D printed designs are often quite open and do allow visual inspection of the skin and wound.

Software algorithm

An algorithm is necessary to convert the scan of the upper limb into a 2D or 3D printable orthosis. This should preferably be automatic or with the least number of manual steps possible. The algorithm has to create a personalised pattern based on the anatomy of the patient.

Appealing design

The cast should preferably have a good-looking design e.g. for kids this could mean nice patterns or colours.

Optional – Allowing flexion of the wrist

One of the major problems with immobilization is the stiffness of the muscles and joints. This could be addressed by allowing flexion of the wrist for stable fractures. During the development of the orthosis, this possible feature should be taken into account. However, since this causes a high amount of complexity to the orthosis it should not be a priority at first.

4 DESIGN

In this chapter, the initial design choices are explained. A flowchart that provides an overview of the implications and limitations of a certain design choice is shown in figure 4.1 below.

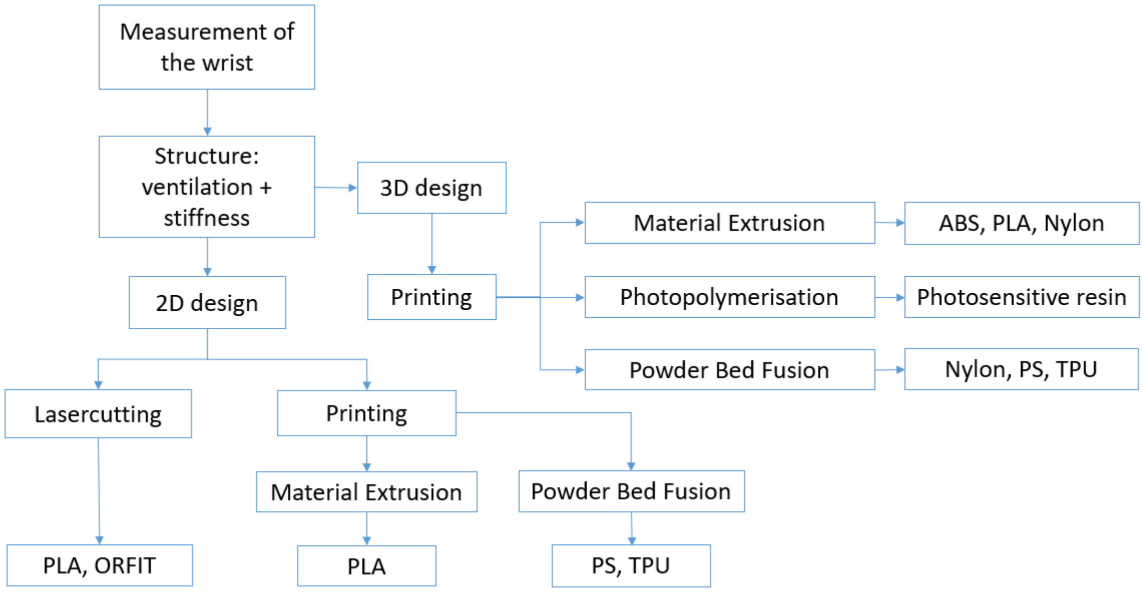

Figure 4.1 Flowchart of design choices

4.1 Fitting – obtaining the shape of the wrist

Current manufacturers often use wrist circumference and standard dimensions to fit an orthosis. This is efficient and produces reasonable results. Another option is a 3D scan of the arm, which will result in a truly personalised orthosis. Companies use low-cost 3D scanners for this task. However, the Rijnstate hospital has investigated 2 different 3D scanners: the Occipital Structure scanner and the Shining 3D. The first has an accuracy of ~3mm and the latter ~0.5mm. A high-quality scanner such as the shining3D is necessary to truly benefit from having a 3D scan of the arm, especially when no small modifications are possible. The issue with the shining3D is that a powerful graphics card is necessary and that it has a small learning curve to be used. Also, during the seconds it takes to obtain a 360-degree image, the limb could slightly move or parts of the limb can be left unscanned. During the period of the thesis, the Einscan was available for a day and other measurements were performed with the Occipital scanner.

4.2 Structure - ventilation and stiffness

Pre-produced (non-)perforated thermoformable orthoses do not increase comfort drastically compared to normal plaster casts. This is because the orthosis is less comfortable without the undersleeve, but also doesn't ventilate significantly more to allow showering and increased wear comfort due to the very small holes. Ventilation can be achieved in different ways. The material can be an open structure by itself or the design of the orthosis can be open such that the skin is in direct contact with the outside air. With a personalised orthosis, it is possible to design a ventilated orthosis. Since open materials tend to be less stiff, it will be easier to use a structure that is open by design instead of open by material properties. Thus, in this thesis is focus will be on designing a structure that is both ventilated and stiff. Common ways are to use a Voronoi or hexagonal pattern, but other patterns can be found as well. Voronoi and hexagonal pattern both have their advantages and disadvantages regarding strength and stiffness. In advance it was unclear which would be more suitable for the use in the orthosis, thus during development, both patterns were used and compared.

The size of the gaps/holes is a balancing equation between stiffness and ventilation. An orthosis with larger holes will provide more ventilation and allow better visual inspection of the skin but will have reduced stiffness. Smaller holes lead to higher stiffness with the same thickness, but reduced ventilation and thus fewer benefits compared to conventional treatment will we provided. In conclusion, the aim was to create the largest holes possible with reasonable stiffness and thickness. As a starting point, the estimated optimal thickness was between 3-4mm based on previously published articles.[27,28] Ideally, an optimized structure is used that is calculated with a finite element model analysis based on the maximum appliable forces. However, this is a time-consuming challenge and was out of the scope of this thesis.

4.3 Speed and production – 2D or 3D design

In the past few years, 3D printers have increased in speed via different printing types. With FDM printers it is a balance between speed and accuracy and the size of the nozzle is greatly important. But some techniques have advanced and use clever tricks to increase production speed while maintaining high accuracy and smooth borders. An example is the Carbon printer which uses resin-based printing with an additional oxygen layer that allows for faster printing. Other manufacturers have come up with similar techniques. The complexity and initial development costs are high with this product. Thus, purchase costs and maintenance costs are significantly higher than conventional production of casts or than production with, slower, FDM type printers. Despite all efforts, printing an orthosis still takes a little over an hour. And additional disadvantages include the toxic state of the resin before it is cured as well as the toxic waste that is produced after rinsing the orthoses. Due to the above-mentioned disadvantages, in this thesis, a different plan of attack is investigated to tackle the speed problem: producing the orthosis flat.

Folding a 3D surface into a 2D plane and back comes with some serious difficulties. Cubes and other straight surfaces can be folded from one piece without much compromise. However, when a surface becomes double-curved such as an hourglass or a sphere many problems occur. This shape can be folded approximately with cuts, but the folded shape will never become perfectly circular. Since the shape of the orthosis is double-curved folding it can either be achieved by making multiple cuts in the 2D plane or by using a mouldable material that is draped and shaped over the wrist. Since cuts decrease the stiffness of the orthosis and do not optimally form around the wrist, a thermoformable material was chosen for the production of the orthosis.

Besides the increased speed, 2D production is less expensive because no support material is necessary and more orthoses can be produced per hour. Additionally, small adjustments can be made on the spot based on patient feedback. However, producing flat has other disadvantages as well. The fact that the orthosis needs to be folded and applied by a technician means that the fit is still partly skill-dependent. Also, fewer printing techniques are available, because thermoformable materials with a reasonably low glass-transition temperature are limited. Additionally, deformation of the material can reduce its strength or stiffness. And finally, in the process of digitally converting from 3D to 2D and physically back again, a lot of details are lost of the first 3D scan. Despite these disadvantages, it is still worth investigating 2D production, because the slow production speed of 3D printing is so restrictive.

4.4 Printing vs laser cutting

The main goal of producing in 2D is to increase production-speed. When comparing 2D printing to laser cutting. 2D printing has the advantages of not producing waste material and that it can print in variable thicknesses. However, the most common printers do not have a large enough print bed to print an orthosis in 2D and post-processing is necessary to smooth the surface. On the other hand, laser cutting can take the speed-increase a step further than 2D printing. The production speed is around 10 minutes instead of 1.5-3 hours with an FDM printed equivalent, there is no need to smooth layers after laser cutting and thus the orthosis can be instantly applied. Another benefit is that most commonly used laser cutters already have a large enough surface area to cut 2D orthoses. The downsides are the slightly higher initial costs (~€11k for a laser-cutting machine, ~€7k for an FDM printer) and that more waste material is produced. For the production, laser cutting is chosen because increasing the speed is crucial for clinical implementation.

4.5 Material

The most important material properties are its rigidity, strength, biocompatibility. However, one of the material properties that is necessary to print the orthosis flat is that the material can be formed around the wrist when it is applied to the patient. A common way to do this is to use a thermoformable material. PLA is an inexpensive material that can both be 3D printed and thermoformed from a flat to a 3D structure. According to the site of Universal Laser Systems[29], PLA does not produce harmful gasses during laser cutting or printing and produces a smooth clean edge when cut. During the testing phase, untreated PLA will be used to limit costs (~€20 per 750 gram), but in the final stages, PLA with additives that make the material bacterial resistant, such as PLACTIVE AN1™ (~€65 per 750 gram), will be used since this is more suitable for clinical use. The material costs for a 52-gram orthosis will theoretically be €1.40 or €4.67 excluding btw and support material. With laser cutting, a material by ORFIT can be used that is based on polycaprolactone, with an antibacterial additive, which is medically approved and is manufactured to stabilize the wrists. This material its costs are, in non-bulk, €142,89 for a sheet of 6 orthoses = €23,82 per orthosis. Based on these properties, initially Fibers sp2020 sheets are used for cutting which cost €34,50 for a sheet of which 8 orthoses can be cut for €4.31.

5 DEVELOPMENT

In this chapter will be explained how the designing choices are translated into practice and which alterations were made during the development to optimize the orthosis. After the wrists were scanned, an algorithm was built to test the chosen material and production technique.

5.1 Fitting - Scanning the upper limb

The input data that is used for the algorithm are 3D Scans of the upper limb that are initially made with the Einscan Pro and Structure scanner with the arm free on the table with the operator walking around 360 degrees while scanning the arm. The arm was held in a neutral position as if it was cast in plaster, thus the fingers not spread and the wrist in 20-degree dorsal flexion. For previous swelling measurements on the wrist, a setup was used to hold the arm stable, however, this blocks the view of the scanner and causes inaccuracies at the fingers thus is chosen to scan the arm free-standing as shown in figure 5.1 below. This does theoretically cause more movement, but the scans were acceptable to use. Some scans showed a stitching error at the starting/endpoint of the 360-degree walk-around but this could be solved by rescanning.

Figure 5.1 STL mesh of the upper limb, scanned with the Einscan pro

5.2 Algorithm

After several programs were tried and compared, Rhino6 in combination with grasshopper was chosen as a software tool. Shown below is an overview of the different steps that are implemented in the algorithm.

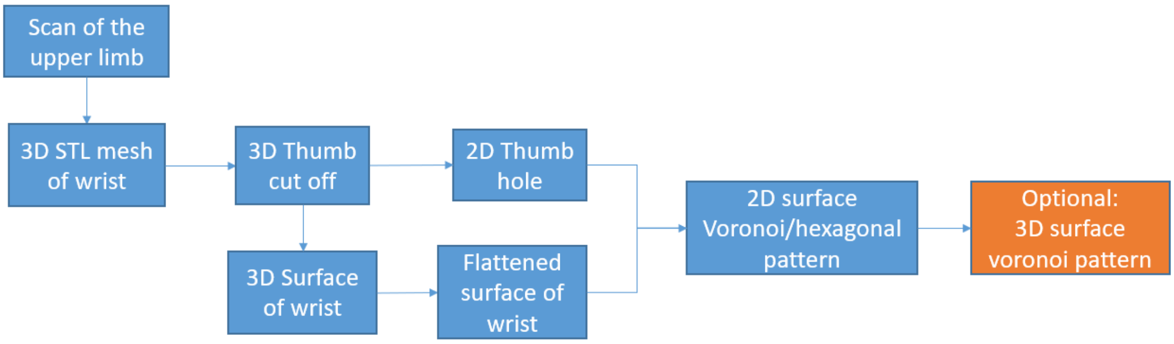

5.2.1 MESH TO SURFACE AND 3D THUMB CUT OFF

At first, direct conversion of the STL mesh file to a surface was attempted via the *MeshtoNurb* command. This step is necessary to generate a Voronoi pattern on the wrist and to use other commands. Unfortunately, with this command, the result is a polysurface, while a surface is required. Thus a different approach was necessary.

Next, an approach was used that was inspired by Li 2018[27]. They use intersection lines that represent the diameter of the upper limb at several distances and then loft them to recreate the surface. A similar technique with the use of contours was used in this thesis as is described step by step below.

Steps that were taken in Rhino6 to loft the surface:

1) *Contour* command was used to draw lines (2-5mm apart) that represent the outer diameter of the wrist. The direction that has to be selected for the contours should be orthogonal to
2) The lines that are not necessary for the orthosis were removed at the proximal and distal end of the arm.
3) When open curves were still present, *SelOpenCrv* command was used to delete them.
4) A plane was drawn at the location of the thumb(hole) perpendicular to the contours.
5) The thumb was cut off with the *split curve* command and the drawn plane
6) Then *closecrv* command was used to close the curves
7) The *loft* command was used to create the orthosis surface with settings tight and 100 curves. Currently, manual selection of the seam is used for better results.
8) Intersectcrv was used to select the lines of the thumb
9) Then the lines are lofted and meshoutline was used to create a curve.

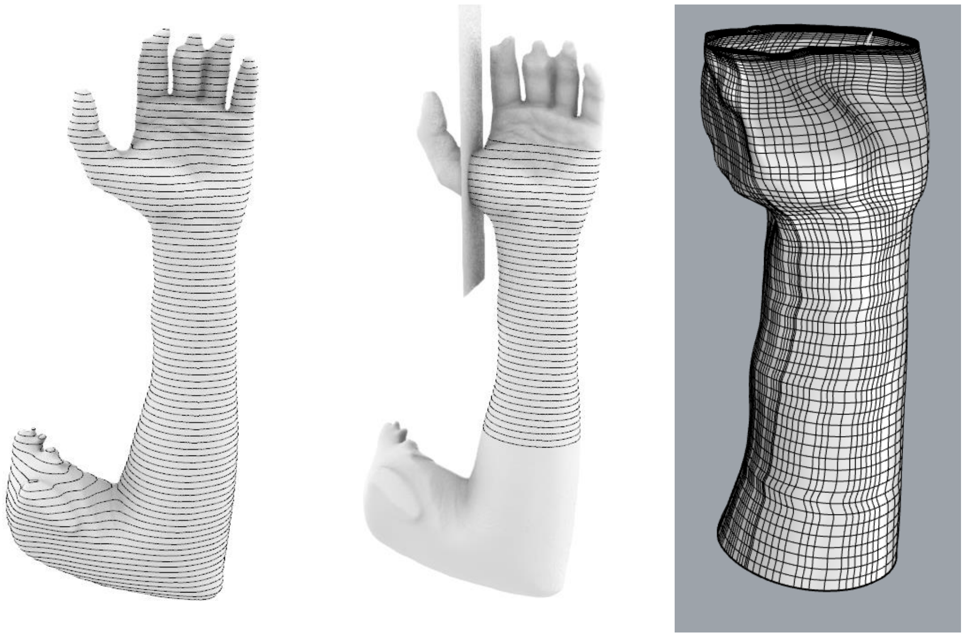

(a) (b) (c)

Figure 5.2 Lofting steps (a) Step 1, (b) step 2-6, (c) step 7

The selection of the direction of the contours is important for the fit on the distal end and the ability to virtually unfold the orthosis. The direction is preferably orthogonal to the line shown in figure 5.3a. Corrections in the distal angle are time-consuming and cause imperfections in the loft (figure 5.3b) which produce unusable surfaces (figure 5.3c). That is why the steps in figure 5.3 are not performed in the final design. Another important detail is that when lofting, *tight* should be selected to obtain a surface instead of polysurface. Also, the rebuild setting introduced some slight deviations between the lofted surface and the contours but these deviations are neglectable when rebuild setting 100 or more is used.

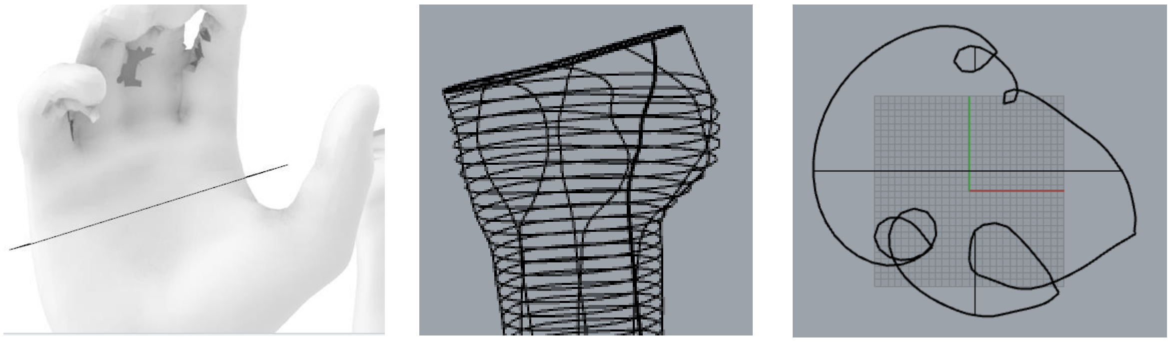

(a) (b) (c)

Figure 5.3 Fit at the distal end of the orthosis (a) in 3D (b) lofted corrected surface (c) unusable unfolded surface

An important step during the loft function is the selection of the seam. The seam determines where the fold will take place and determines the shape of the flattened surface. The location of the seam is preferably at the location of the ulna for 3 reasons. Firstly, the smallest width direction is chosen because the orthosis can then be put on and taken off more easily. Secondly, the closing mechanism is a potential weak point, thus the largest forces are preferably absorbed by a uniform piece of the orthosis instead. Finally, the mechanism should not be on the side of the radius because in that case stability of the thumb would be more difficult to accomplish and the side of the fracture should be relieved as much as possible.

The different seams are shown in figure 5.4 on the surface of the wrist. Automatic seam generation usually results in a smooth seam (figure 5.4a), however, the seam is not in the right position at the ulna. When moving the seam with the automatically generated points, a seam is formed that does not follow the desired path (figure 5.4b). Thus, for now, a manual selection (figure 5.4c) is used to make sure the seam does not compromise the design. However, manual selecting all the seam points is cumbersome and should be automated before clinical application. A few pages below in figure 5.7, the consequences of manual and automatic seams are shown in their flattened state.

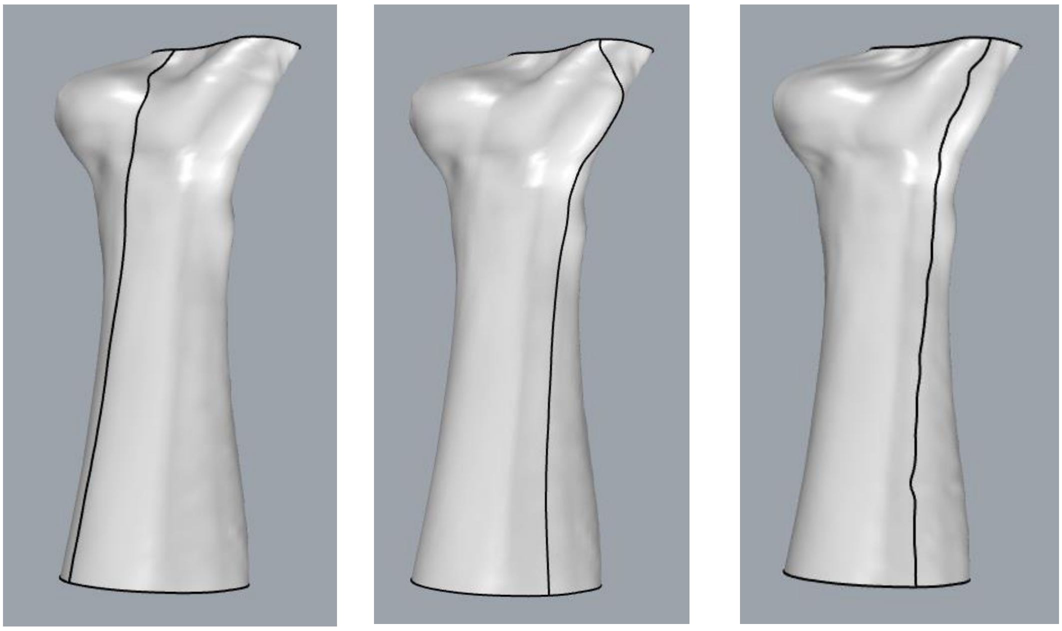

(a) (b) (c)
Figure 5.4 The seam of the surface; (a) automatic seam (b) shifted automatic seam (c) manual seam

5.2.2 THUMBHOLE

Initially, the Voronoi pattern was processed without a thumb hole in 3D to then later be removed in 3D space because this way you could visualize the location of the thumbhole of the orthosis on the wrist and visually make adjustments in 3D space. However, it is difficult to create the hole in 3D space and conversion from 2D to 3D is computationally heavy. Also, 3D to 2D commands do not work anymore with the pattern already formed. That is why the thumbhole is removed in 2D at a standard position, but can still be checked in 3D space when desired.

The cut-off thumb has to be converted to 2D space as well. Initially, an oval was drawn that approximated the size of the cut-off area based on the view as shown in figure 5.5 on the next page. Later, this area was determined automatically which is rebuild to a lower polynomial shape as shown in figure 5.6 The lower polynomial shape is used to soften sharp edges that would be uncomfortable when the thumb slides over them. However, the automatic shape did not yet deliver the desired size and shape and should be improved further before being used.

Figure 5.5 Side view of thumb with the outline of the area used as thumbhole

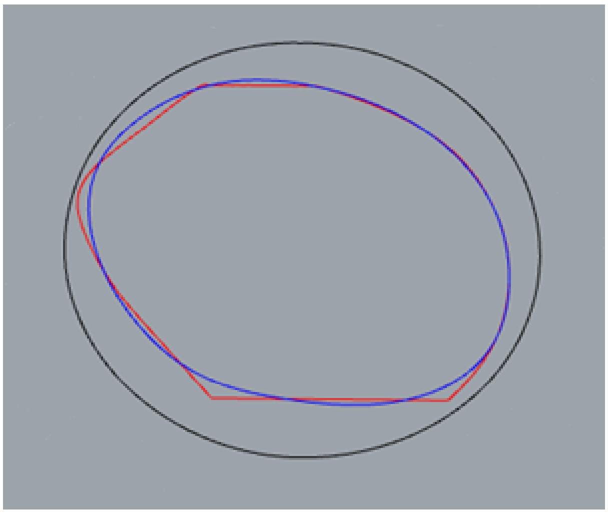

Figure 5.6 2D curve of the thumbhole, black: manual selected, red: automatic generated, blue: rebuild automated thumb hole

5.2.3 3D SURFACE TO FLATTENED SURFACE

After the mesh is converted into a lofted surface, the surface can be flattened. As discussed in chapter 4.3, converting a 3D surface to a 2D plane is intertwined with a lot of difficulties. Most algorithms such as *smash* and *unrollsurface* are not capable of a 3D to 2D conversion with double-curved surfaces. However, the command *squish* can handle this and, thus, is the used command in this thesis.

After the surface is lofted in steps 1-9 in paragraph 5.2.1 the following steps were taken in grasshopper:

10) The limb-surface without thumb is expanded with the *offset surface* module in grasshopper 1mm to allow breathing space for the skin
11) *The Squish* command creates a folded 2D shape of the expanded 3D arm
    a. The seam determines the shape of the flattened curve
    b. The expansion of the surface determines the size and shape of the flattened curve
    c. The anatomical position of the wrist determines the shape as well

As pointed out in paragraph 5.2.1, the position and shape of the seam determine the shape of the flattened curve. In figure 5.7 the manual seam on the ulna is shown in black and in yellow the automatically generated seam that is located on the ventral side of the wrist. A clear shape difference is shown, but unfortunately, it is not always clear whether the seam on the ulna will also accomplish the best fit in practice. In figure 5.8 the influence of the expansion from the skin is visualised for 0, 1 and 3mm. It is visible that the shape of the flattened orthosis is moving towards a more rectangular shape. For a still unknown reason, the curves do not always produce the same consistent shapes for other wrists, which could be a potential problem when applying the algorithm to different patients.

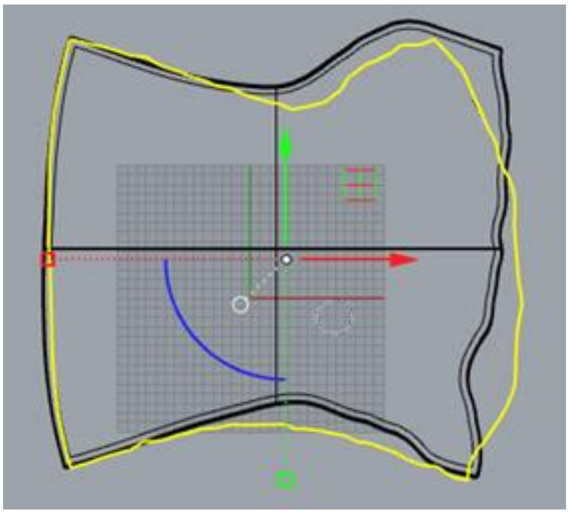

Figure 5.7 Flattened surface of the wrist; Yellow: manual seam on the ulna, black: automatic seam between the radius and ulna

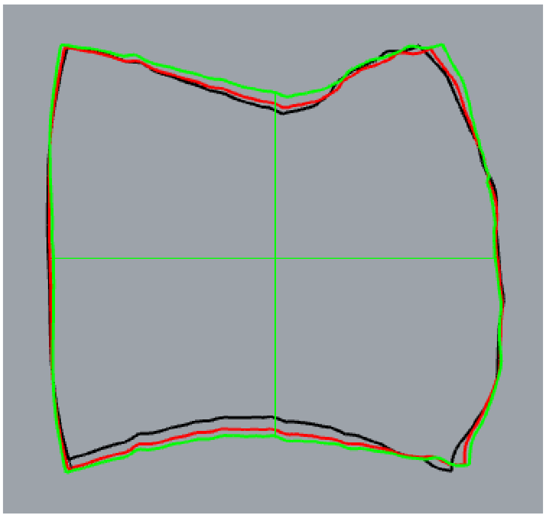

Figure 5.8 Flattened manual seam surface of the wrist; Black: 0mm-, red: 1mm-, green: 3mm expansion

The settings that were used for the squish command were splitseams= Yes, preserve boundary=No, deformation=Free, material=Floppy, Outside=up, Decorate=no. Split seam should be yes for a single surface and no for a polysurface, however, it does not change the output when tested during development. Preserve boundary makes sure the boundary is the correct length but does distort the boundary's geometrical shape as seen in the cyan line in figure 5.9. The deformation setting changes whether the priority is given to prevent stretch, compression or that it can do both (setting: free). The setting changes the surface area that is produced significantly as shown in figure 5.9 where the centres of all the surfaces are in the same point and thus the compress mostly (magenta) line clearly shows a larger surface area than the stretch mostly (blue) line. The material setting can be floppy or rigid, rigid is to minimize stresses on the material when bending, while floppy limits geometric distortion as much as possible. The decorate function places small red and green dots that correspond with the 3D structure for comparison.

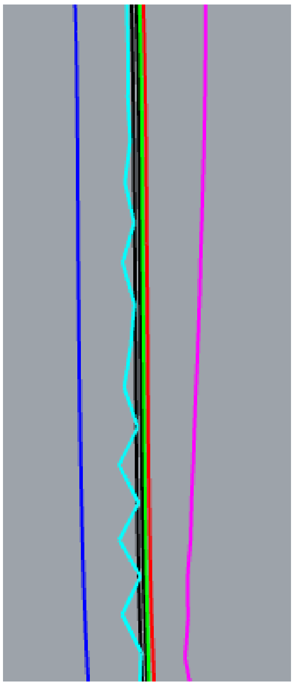

(a)

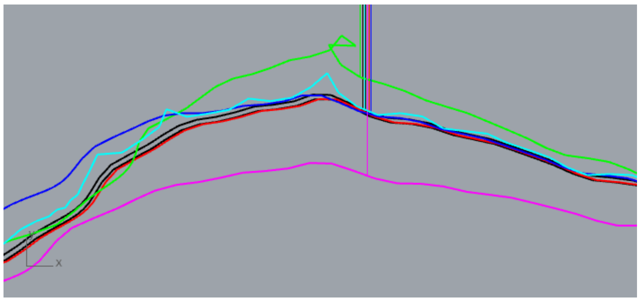

(b)

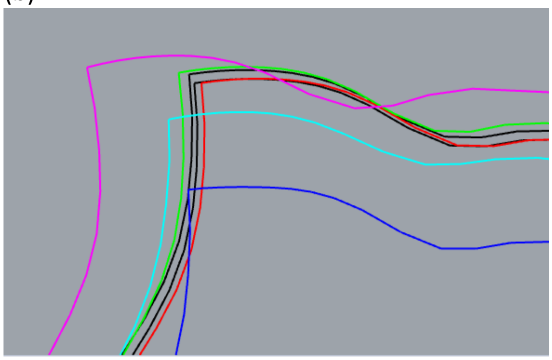

(c)

Figure 5.9 Different squish settings; magenta: compress mostly, green: rigid, cyan: preserve boundary on, blue: stretch mostly; (a) right middle (b) middle-bottom (c) left top corner

5.2.4 CREATING THE VORONOI PATTERN

During the design phase, it was not clear which pattern would be most suitable for the orthosis. It depended on the possibilities that would be available in the algorithm such as attractor options, density, distribution. Below, the size and complexity of the algorithm is shown. The Voronoi pattern has a fast and clean algorithm that has the option to be further developed as a 3D printed design.

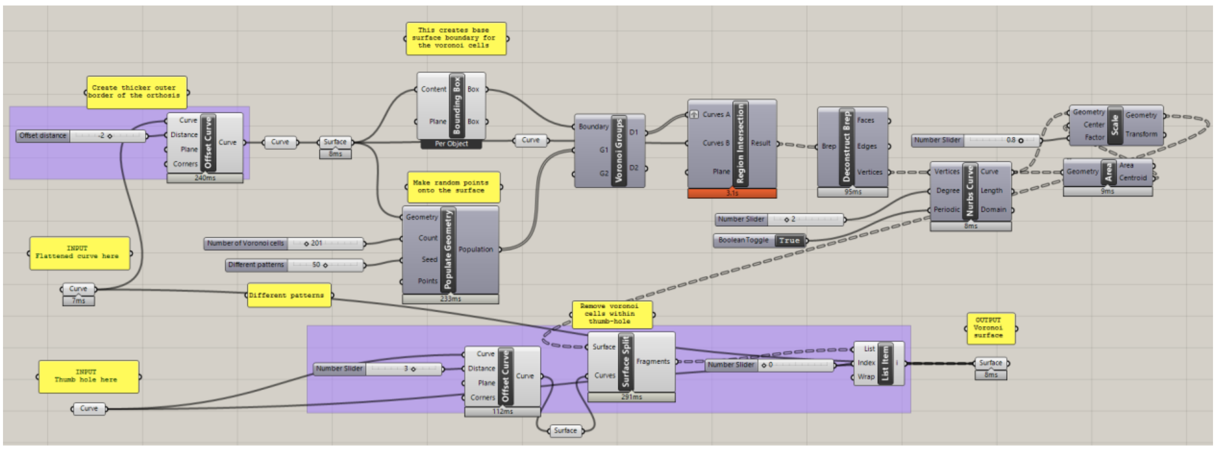

Figure 5.10 Grasshopper Voronoi architecture

Creating the Voronoi pattern with Grasshopper:

1) Offset curve was used on the squished surface to create a boundary box with a thickness of the boundary of the orthosis (red line in figure 5.11a)
2) Random points were created within the offset curve by using the command populate geometry. The count parameter changes the amount of Voronoi points, the seed changes the arrangement of the points randomly.

   a. Optional: an attractor is used to create extra Voronoi points in a certain area that needs more strength (figure 5.12)
3) Voronoi groups were created based on the created points combined with a created boundary box which is based on the offset curve (fig 5.11b)
4) Nurbs curve is used to create the roundness of the Voronoi cells. This creates a more natural strength in the corners since those are usually the weakest link in the structure. (fig 5.11c)
5) The surface of the thumb is offset with 2 or 3 mm to create extra strength around the thumb hole
6) This offset curve is used to split the Voronoi cells that are positioned around the thumb hole (fig 5.11c)
7) Finally, the thumbhole is cut out of the 2D structure (fig 5.11d)

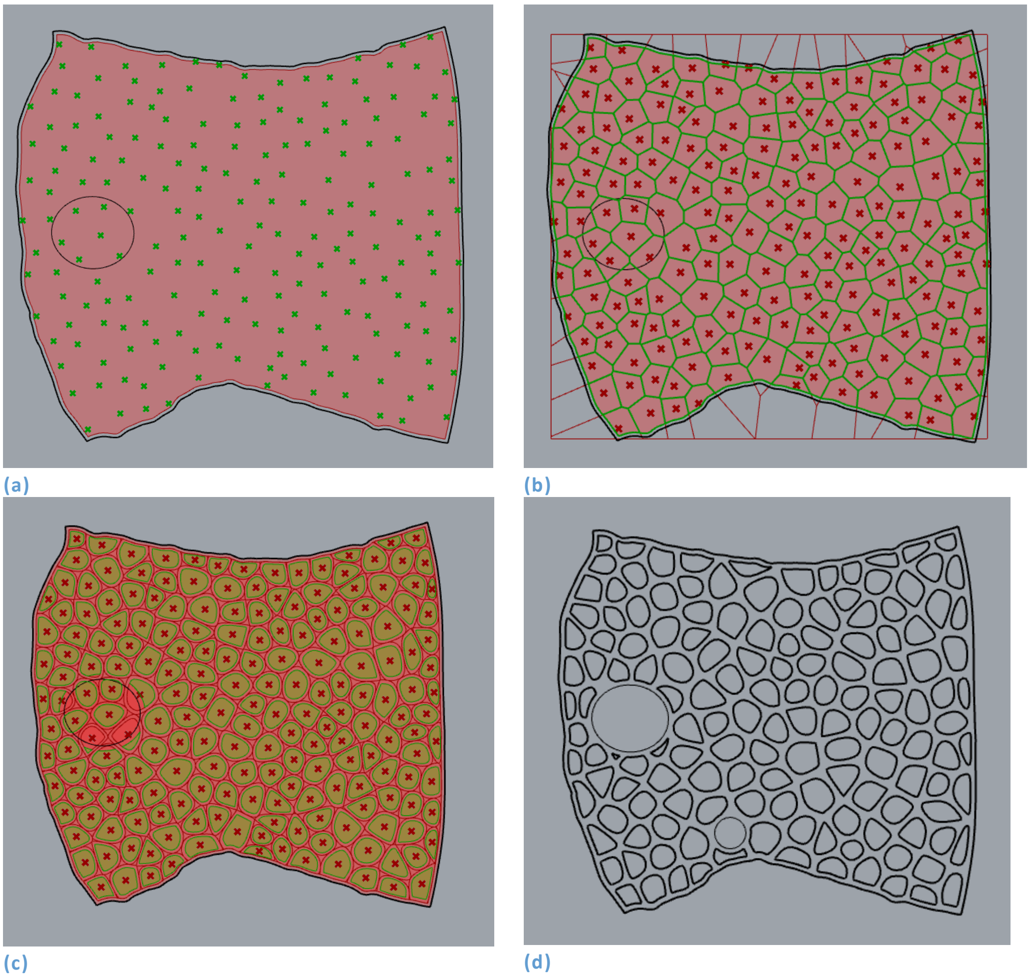

Figure 5.11 Process of creating the Voronoi pattern (a) step 1 and 2 (b) step 3 (c) step 5 and 6 (d) step 7

Optional - Attractors

First, the attractor was used to increase stiffness at the location of the fracture, because the forces are highest at this location. However, this caused some issues with the PLA because the PLA was less shapable than previously thought and the bulges at this location need sufficient flexibility of the material. Thus the decision was made to experiment with and without attractors to find out what produced better results.

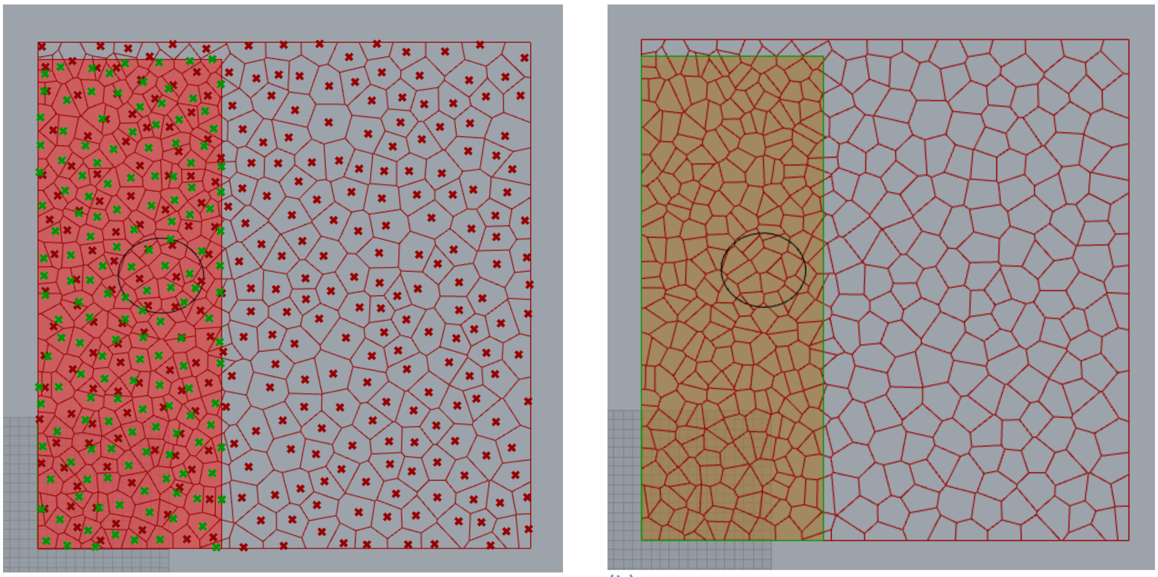

(a)

(b)

Figure 5.12 Bounding box Voronoi pattern; (a) green dots: additional points created by attractor (b) regrouped Voronoi points after including the attractor

5.2.5 VORONOI PATTERN 2D->3D

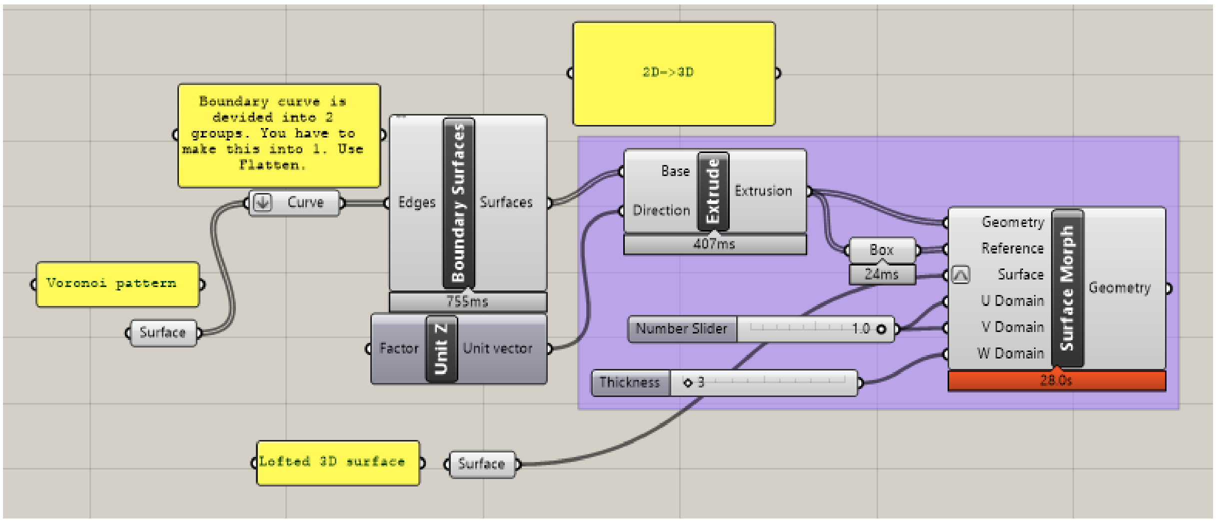

Figure 5.13 2D to 3D projection

In order to visualise the Voronoi pattern on the wrist, a 2D to 3D module is implemented in Grasshopper. The input is the surface output of the generated Voronoi pattern and the lofted 3D surface of the wrist that was created before. The W domain determines the thickness of the orthosis. This module can also be used to test or compare a 3D printed variant to the 2D variant.

Figure 5.14 3D visualisation of the Voronoi pattern

5.3 Creating the Hexagonal pattern

Below, the overview of the grasshopper network of the hexagonal pattern is shown that was developed parallel to the Voronoi pattern. The input data is the squished surface, the 2D shape of the thumbhole and optionally a hole for the processes ulnae that specifically reduces pressure on a protruding structure. The green area is the attractor, the orange area creates thickness for the border of the orthosis itself, the thumbhole and optional hole for the ulnar styloid process. The red area is the conversion of a 2D plane back to a 3D visualisation of the orthosis on the wrist.

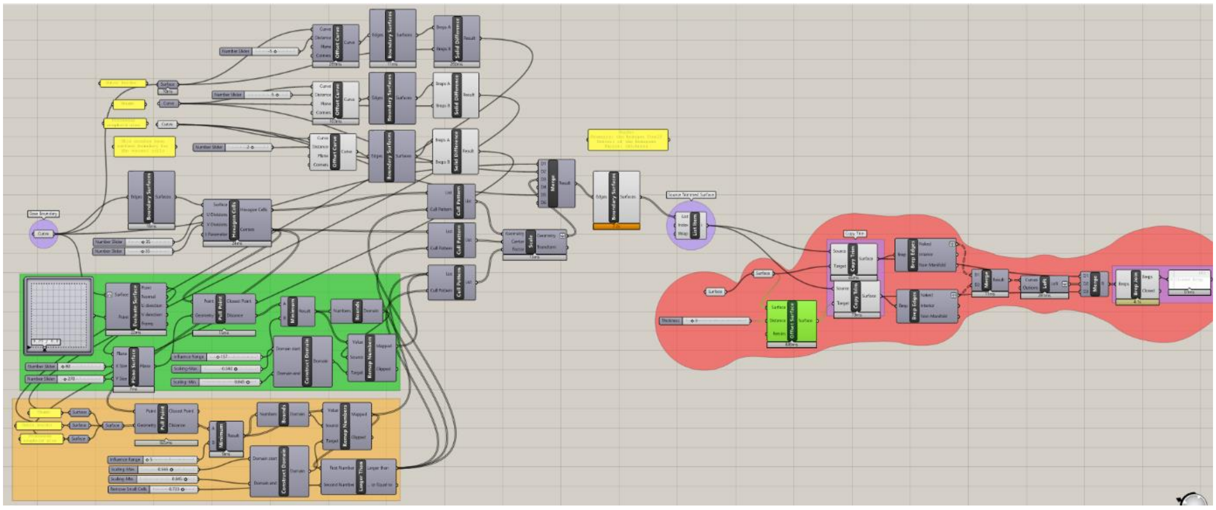

Figure 5.15 Grasshopper hexagonal pattern architecture – a complete overview

1. The squished curve was used as input data and converted into a boundary surface
2. The boundary surface was fed into the hexagon cells with U and V dimensions of ~35 hexagon cells depending on the thickness and necessary strength. Fewer hexagon cells caused either

glitches or large parts covered instead of ventilated which is one of the reasons why the Voronoi pattern was preferred over the hexagon pattern.

3. An attractor is used to increase the density at the distal end of the orthosis. Contrary to the Voronoi pattern, this was created with a smooth transition of larger cells to smaller cells from proximal to distal that can be regulated by the influence range.
4. The thickness of the borders of the hexagonal cells is set by scaling max and min on a range of 0 to 1 in the construct domain module which were set at 0.592 and 0.845 respectively.
5. The boundaries of the thumb and processes ulnae were used to create holes and a special module was built to thicken the borders, which uses the same parameters as the attractor with an additional feature that removes small cells (set at 0.723) to create a glitch-free correct border.

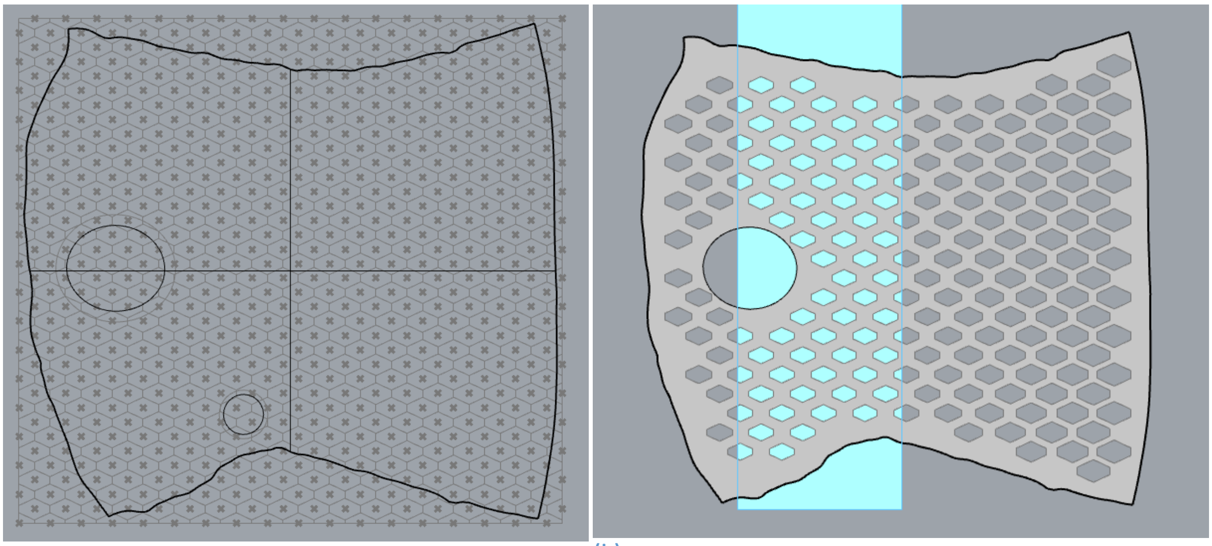

(a) (b)

Figure 5.16 Flattened surface of the wrist (a) step 1-2 (b) step 3-5

5.3.1 HEXAGONAL PATTERN 2D->3D

For the hexagonal pattern, a different way is used to convert the 2D shape into a 3D shape. By using Offset surface, loft and Brep-join as visualised in figure 5.17 below. The end result is shown in figure 5.18.

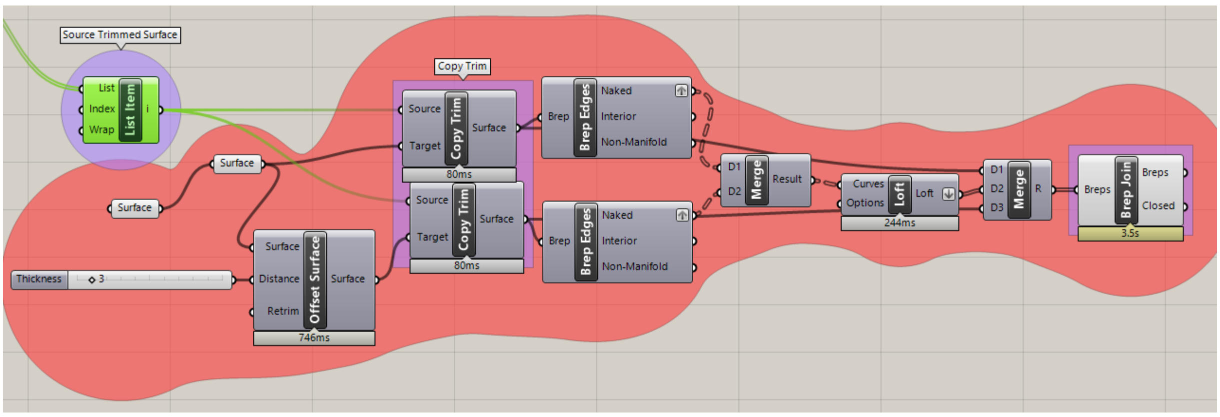

Figure 5.17 Overview of 2D to 3D grasshopper algorithm

Figure 5.18 3D visualisation of the hexagonal pattern on the wrist

5.4 Material – fitting and cutting

During development and testing difficulties with the used PLA sheets emerged. During the cutting of PLA, unpleasantly smelling smoke is released. The smell takes a few days to lower to an acceptable level. This was especially the case with PLA infused with elephant grass. Later, the 'pure' variant was used that was expected to perform better. However, with both PLA types ugly visual burn marks are visible which also transmit to the skin both on the cutting lines and the location of the metal grid it is cut on. Another disadvantage of the PLA sheets is that they are not sufficiently flat for being processed well in the laser cutter. Wobbles in the material caused imperfections in the cut.

Initial tests with the PLA do not show a proper fit around the wrist because the material was not as flexible when heated as expected. Next, an alternative material was used to continue testing instead. This was the medically approved material which is already used for wrist orthoses from a company called ORFIT. The advantages are a better mouldable material that smells significantly less after cutting and the sheets are perfectly flat. Also, no profound burn marks are visible and skin contact is tested for safety. Unfortunately, this material is more expensive and increases raw material costs 3-4 fold compared to PLA.

5.5 Closing system

For the closing system, a temporary solution is used during the testing phase. This consist of a few metal garbage wires that can be braided between the orthosis which stiffened the construction sufficiently. When trying Velcro to secure the orthosis, noticeably more pressure was exerted on non-comfortable places, in contrast, tightening it was significantly quicker.

6 VALIDATION METHODS

6.1 Stiffness

At first, an attempt was made to calculate the stiffness of the orthosis with a virtual model. The program Fusion 360 was used for this purpose. However, the strength calculations were not well suited for a curved open structure such as a Voronoi pattern. The maximum number of vertices was 10.000 (later updated to 20.000) to perform calculations but the shape of the Voronoi pattern was not representative anymore and caused self-intersections because of a reduction factor of 63 (98%) as seen in figure 6.1 and figure 6.2.

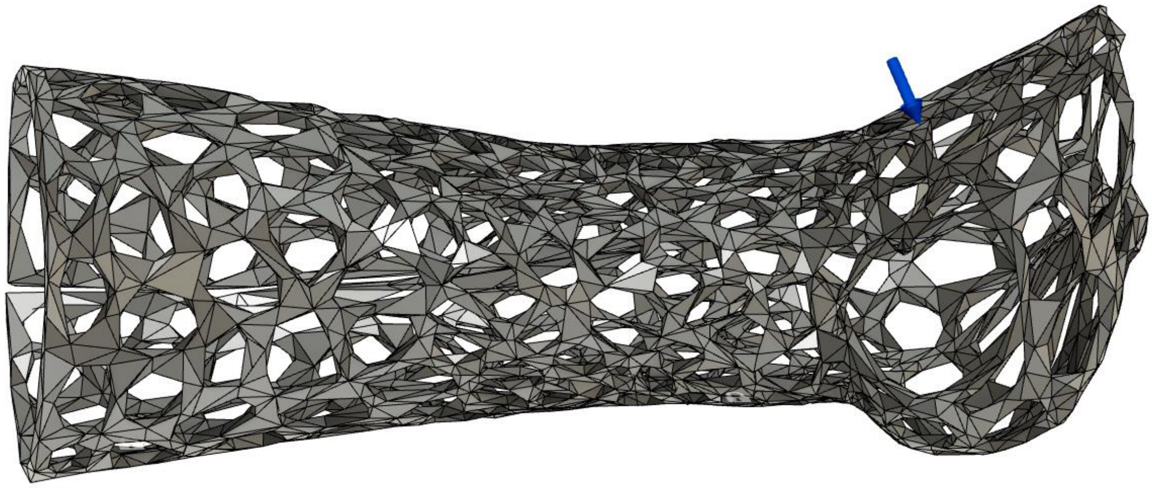

Figure 6.1 Remeshed orthosis: 10.000 vertices

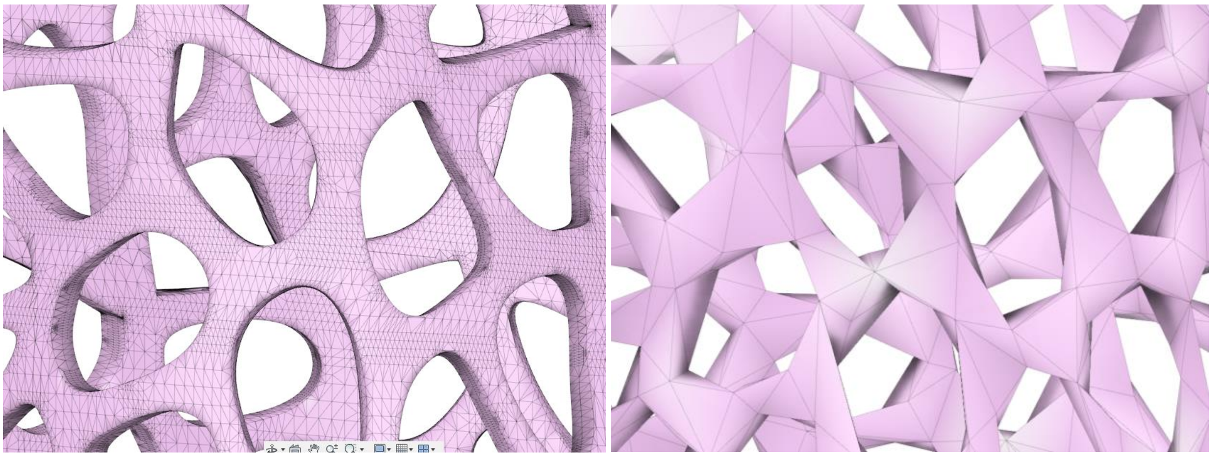

(a) (b)

Figure 6.2 Close-up of mesh (a) original: 626.892 vertices (b) remeshed: 10.000 vertices

6.1.1 PRACTICAL TEST

Because virtual strength and stiffness tests have their limitations, practical tests were performed. At first, the stiffness was subjectively tested by trying to bend the material. 1 and 2 mm thick PLA appear not to be strong enough for fracture treatment, but 2mm may be used as a splint. The 3mm PLA and the 3,2mm ORFIT material seem adequate stiff to stabilize a fracture. Then, these expectations were objectively tested according to the test design of van Nieuwenhof 2020[30] which was produced in consultation with the author of this thesis.

The goal of the practical test is to compare the stiffness of the produced orthosis with a conventional plastic cast. There are several ways to measure stiffness, the most commonly used being the 3-point- and a 4-point flexural test. This is a consistent and reliable test, however, this method does not take into account the shape and design of the orthosis. That is why it is attempted to create a more realistic load scenario to measure the stiffness by using a cantilever bending test. First, measurements were performed for the force that a strong healthy male could exhibit on an orthosis by flexion and extension. This load was then applied to the conventional treatment cast in an experimental setup that represents actual forces on the orthosis. A PLA phantom was used that represents a wrist printed by van Wijk2019[31] which includes a hinge at the wrist and a slit that represents a DRF. The phantom was scanned with the occipital scanner and the orthosis tailor-made with Rhino6 and grasshopper based on this scan. The orthosis was moulded around the orthosis using an 80-degree Celsius water bath and closed using several metal wires. Additionally, a coiled metal wire was placed in the slit that acts as a hinge and can provide a standard gap distance. The metal wire was used instead of a magnet ball due to material availability.

The curvature of the orthosis is measured by using x-ray screening with the MultiDiagnost Eleva with Flat Detector (Philips Medical Systems, Best). The phantom with the orthosis is placed in a wooden construction that stabilizes it and has a support just proximal of the fracture. The weights are loaded according to the setup of van Nieuwenhof2020 from 0 to 12 kg. The weights were hung with a string 3cm distal of the wrist hinge in both flexion and extension separately and are counterbalanced by thick Velcro strapped to the table. The curvature of the orthosis is measured by assessing the difference between the starting angle and the angle with the load applied as visualised in figure 6.3. Figure 6.3 shows the orthosis around the phantom as well as the lead strip that was previously used to determine the angle by van Wijk, that was later substituted by measuring the gap angle by van Nieuwenhof because of consistency. Additionally, the large black surface in figure 6.3 is the table that unfortunately could not be positioned differently.

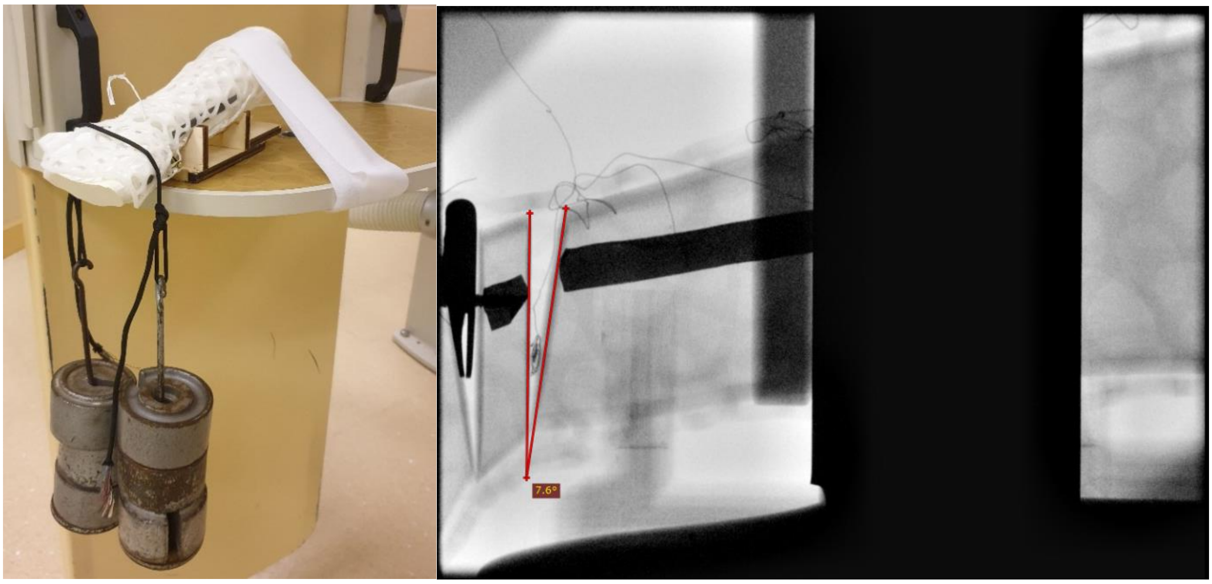

Figure 6.3 test setup of flexion with 12 kg of weights left: visual setup; right X-ray image of the setup

6.2 Testing fit and comfort

The fit and comfort were tested on 2 healthy volunteers. One volunteer's wrist was scanned with the Einscan Pro 2X and the other with the occipital scanner because of availability. Both scans were processed in Rhino6 and grasshopper and a personalised orthosis was laser-cut out of ORFIT material sheets. The orthosis was then heated in an 80 °C water bath and folded around the wrist. Next, the orthosis was moulded around the wrist to have a proper fit until it was cured. The orthosis was worn until discomfort started to occur which was after around 3 hours. After that the orthosis was assessed according to the following validation parameters with a scale of 1 to 10. 1 meaning very dissatisfied, 10 meaning very satisfied.

Validation parameters:

- Overall satisfaction
- Fit (tightness)
- Ventilation
- Itchiness
- Maceration of the skin
- Pressure sores
- Comfort during application
- The appearance of the orthosis
- Solidity
- Movement/stiffness/support
- Closing system

7 TEST RESULTS AND EVALUATION

7.1 Stiffness

For the theoretical evaluation, the measured flexural modulus of an MDO student-group[32] and Mihalko1989[33] is compared to the manufacturer's product specifications. It should be noted that the stiffness values differ strongly among papers[34] and are also tested differently. The student-group performed a 3-point flexural test on two different materials: Cellona plaster bandage from Lohmann & Rauscher for the mineral cast and Delta-cast Conformable from BSN for the plastic cast. The tests were performed by wrapping the material around a wooden plank. The flexural modulus was measured with a 3-point flexural test and the results were 255 MPa for the mineral cast and 64 MPa for the conventional fibreglass cast. Mihalko1989 performed 4-point flexural tests and found different values, in table 1 the results of the papers are summarised. The differences are large and unfortunately, additional data does not clarify or strengthen the values. However, the absolute values of Mihalko appear to be more accurate. For the plaster casts, the stiffness ratio plaster-cast/plastic cast of the MDO study is used, since this should represent clinical practice in the Rijnstate hospital. According to the site of ORFIT, the AQUAFIT NS Stiff material has a flexural modulus of 565 MPa. The thickness of the orthosis is 3.2mm and plaster casts are between 4 and 7 mm. The average amount of (width) reduction from the Voronoi pattern is 2.36 (58%), measured by comparing the weight of the closed orthosis (170 gram) with the open orthosis (72 gram). For the hexagonal pattern, this reduction is 44% compared to a closed orthosis.

Bending stiffness
$$K = E * I \tag{7.1}$$

The area moment of inertia (tube)
$$I = \frac{\pi(D^4 - d^4)}{64} \tag{7.2}$$

The area moment of inertia (rectangle)
$$I = \frac{b * h^3}{12} \tag{7.3}$$

Equation 7.1 shows the bending stiffness. E is the Young's modulus (in MPa), while I is the second moment of area (in m^4). In order to estimate the stiffness of the personalised orthosis, the thickness and the pattern difference have to be taken into account. In equation 7.2 the area moment of inertia is shown for a tube; D is the outer diameter of the tube/orthosis and d is the (inner) diameter of the tube/wrist. The wrist circumference is expected to be between 12.5-21 cm (diameter=39.8-66.8 mm) ranging from a small woman's wrist to a large man's wrist. Based on this equation, for adults, the expectation is that a 4mm- thick orthosis will be 31% stiffer than a 3.2mm-thick orthosis. When the inner diameter becomes smaller, the stiffness difference increases. E.g. for a 6-year-old girl with a wrist circumference of 10.5 cm the difference becomes 33.9%.[35] The personalised orthosis is reduced in width as well due to the Voronoi pattern, which is linear according to equation 7.3. The Voronoi pattern reduces the width with 58%, so the orthosis will be at least 2.36 times less stiff than a completely closed orthosis. As shown in table 2, combining the material property, thickness and design the expectation is that the orthosis will be more than 1.74 times less stiff than a fibreglass cast. The plaster cast and 5.0mm thickness are added for comparison. Although the plaster cast seems superior in stiffness, it should be noted that the resistance to breaking of this cast is lower than for the plastic casts.

Table 1 Flexural modulus overview

	Flexural Modulus Mihalko1989 (MPa)	Flexural modulus MDO group (MPa)
Plaster cast – low dens (4mm)	1747.9 ± 1030	-
Plaster cast – high dens (4mm)	2590 ± 708	-
Plaster cast – (6.8mm)	1264 (estimated)	255
Conv. Plastic cast (3-layers)	316 ± 15 (5mm)	64 (3.9mm)
ORFIT cast (manufacturer spec.)	565	565

Table 2 Theoretic stiffness comparison

Thickness	3.2mm	4mm	5mm
Plaster cast (1264 MPa)	3.05x stiffer	4.0x stiffer	5.28x stiffer
Plastic cast (316 MPa)	1,31x less stiff (24%)	**baseline**	1.32x stiffer
ORFIT cast (565 MPa)	1.37x stiffer	1.79x stiffer	2.36x stiffer
Pers. ORFIT cast (565 MPa)	**1.73x less stiff (42%)**	1.32x less stiff (25%)	Same as baseline

7.1.1 PRACTICAL TEST

The results of the bending test of Nieuwenhof 2020[30] were compared with the results of the validation tests performed in this thesis. A selection of the results is shown in table 3, additional results can be found in table A-1 in the appendix. The flexion and extension values of van Nieuwenhof are converted from radians to degrees and the net angle is calculated. The bending of the personalised ORFIT orthosis under flexion had 3 and 4 degrees difference with 12 kg compared to 0 kg which was 5.0-6.7 times larger than the measured value of Nieuwenhof for the conventional fibreglass cast. For extension approximately an 8- or 9-degree difference was measured and this was 4.7-6 times higher than was found for the fibreglass cast. The values of the extension are higher than the flexion for both the personalised ORFIT orthosis and the conventional fibreglass cast. Since the orthosis is loaded at the same distance as the setup of Nieuwenhof, the angles can directly be compared and translated to stiffness. Thus the measured stiffness of the personalised ORFIT orthosis is approximately 5 times less than of a 4mm fibreglass cast.

Table 3 Direct bending comparison

Flexion pers. ORFIT	Load	Degree Angle	
		Total	Net
ORFIT-F0	0 k g	0,0	0,0
ORFIT-F1	4 kg	2,3	2,3
ORFIT-F2	8 kg	2,6	2,6
ORFIT-F3	12 kg	3,0	3,0
Flexion - van Nieuwenhof - 3 layers			
FIBRE-F0	0 k g	13,6	0,0
FIBRE-F1	12 kg	13,0	-0,6
FIBRE-F2	24 kg	12,7	-0,9
FIBRE-F3	32 kg	12,4	-1,2

Extension pers. ORFIT	Load	Degree Angle	
		Total	Net
ORFIT-E0	0 kg	5,7	0,0
ORFIT-E1	4 kg	6,4	0,7
ORFIT-E2	8 kg	11,6	5,9
ORFIT-E3	12 kg	14,8	9,1
Extension - van Nieuwenhof - 3 layers			
FIBRE-E0	0 k g	14,4	0,0
FIBRE-E1	12 kg	15,9	1,5
FIBRE-E2	24 kg	17,8	3,4
FIBRE-E3	32 kg	19,6	5,2

7.2 Comfort of the cast - User reviews

The comfort of the cast was rated according to the validation criteria and the results are shown in table 4. Due to discomfort, both volunteers stopped wearing the orthosis after approximately 3 hours. The bottleneck was the size and shape of the thumb hole, which limits blood flow to the thumb and leaves marks in the skin after a few hours of wearing. During the 3 hour period, the remaining part of the orthosis is perceived as a comfortable fit. After the orthosis became wet, maceration of the skin did occur. The orthosis should be tested for a longer wearing period to test all the validation factors adequately.

Table 4

	Volunteer 1	Volunteer 2
Overall satisfaction	8	7 (comfort thumb)
Fit (tightness)	9	9
Ventilation	9	9
Itchiness	9	9
Maceration of the skin	7 (after getting wet)	8
Pressure sores	6 (mainly the thumb)	5 (thumb)
Comfort during application	7	8
Appearance of the orthosis	9	9
Solidity	9	8
Movement/Stiffness/Support	9	8
Closing system	7 (seam does not always connect properly)	7

8 DISCUSSION

The goal of this thesis was to develop a method to quickly manufacture a personalised orthosis for distal radius fractures. Also, an algorithm had to be developed to create an orthosis because no open- source algorithm was available. Different options were considered but eventually, it was decided to produce the orthosis by laser cutting out of a thermoformable plastic material which is then to be folded around the arm. With this method, finish smoothness and speed can be combined with relatively low cost. The hypothesis was that producing an orthosis flat by laser-cutting would speed up the production process. As expected, the results indicate that laser cutting an orthosis is significantly faster than printing a 3D orthosis. The algorithm is able to produce a personalised 2D drawing that can be laser-cut, but manual corrections are still necessary that require time and skill. Automatization of the size and shape of the thumbhole was not constant enough to replace manual selection yet. In short, the most important problem of 3D printing personalised orthosis is tackled, but some new difficulties have emerged that should be further improved before the orthosis can be clinically implemented.

Orthoses have been produced flat before, but using laser cutting to produce orthoses more quickly has not. Another novelty is that little research is performed comparing the conventional fibreglass cast with a personalised orthosis. Santoni2017 compared a thermoformable Exos brace with a traditional fibreglass cast by using cadavers and concluded that thermo-formed braces were equally stiff.[36] However, they did not use a personalised orthosis, thus the results are difficult to compare. Also, Hoogervorst 2019 conducted a biomechanical comparison of a fibreglass cast with a 3D printed open-latticed cast made out of Nylon 12 and found that those were equally stiff as well.[37] But in this case, it should be noted that the pattern is significantly less open than the Voronoi pattern used in this thesis and a different, more expensive, material is used. Thus it is difficult to compare these findings. The developed algorithm is similar to Li2018 which showed that using CAD modelling software should be suitable for clinicians[38]

In comparison to other papers in which an orthosis was developed, the method in this thesis used a more realistic load scenario. Ideally, a cadaveric arm is used to test fracture movement, since this allows all the joints, muscles, tendons and flexibility of the skin to be taken into account. Also, as discussed in van Nieuwenhof, the force is preferably applied on the orthosis internally via the phantom instead of applying the load externally on the orthosis itself. The used X-ray device was not ideal since the setup had to be rotated compared to the table and another part of the table was blocking the image, using another device could produce a little more precise results and make it easier to perform the measurements. The comfort of the orthosis was evaluated by 2 volunteers for 3 hours. This provides limited data for some of the validation factors. The performed stiffness test was compared with a limited amount of literature, which did not show consistent values.

The results indicate that stiffness of the orthosis is less stiff than a fibreglass cast as was predicted with the amount of reduction from the Voronoi pattern. The difference was however larger than expected based on the flexural modulus and the thickness. This could be caused by the closing mechanism which shows shearing under large tension. However, it can be discussed whether the stiffness has to be that high for non-displaced fractures since small movements can increase callus forming and the most important function of the cast is pain relief.[11,22] The stiffness in flexion was higher than for extension which may be caused by the way the phantom is set up since this occurred with the conventional fibreglass cast as well. The way the orthosis is arched and the direction of the fracture could have contributed. However, this does represent the shape of a human wrist and distal radius fracture. Unfortunately, it would have rather been the other way around since more flexion could be allowed in the wrist without distorting fracture treatment.

The comfort of the orthosis was evaluated by 2 people and was perceived as comfortable except for the fit at the thumbhole. Determining the correct size of the thumbhole is a difficult task because it is not always clear how the thumb is going to fit when it is folded around the wrist.

8.1 Future perspective

A few ideas were beyond the scope of this thesis but should be considered or improved. The author has automated several steps in the developed algorithm. However, a few manual steps remain and knowledge of Rhino6 is still necessary. That is why for clinical implementation, further automatization steps are necessary. Introducing the scanner of Manometric could simplify and solidify this automatization since the scans are at this moment not consistent enough to automize directly. The squish command should be looked into because the 2D shape does not always produce consistent results. The comfort at the location of the thumb should be improved by shape and size optimization of the thumb hole and extra padding should be added such that the orthosis no longer restricts blood flow or causes pressure marks. A finite element analysis could be performed to adjust the pattern based on forces that act on the orthosis. This could reduce the weight of the orthosis or improve the stiffness of the weaker parts.

The closing system is in a pre-production state. The wiring system is easily adjustable but a more robust and pleasing design is necessary to be clinically implemented. One way to improve the closing system and improve the stiffness could be to roughen the border by creating a sawtooth structure that can fit into each other but this does increase the width of the border and thus increases the weight. It will also make it more difficult to line-up the orthosis properly thus it should only be if other alternatives do not suffice. Also, it should be investigated to what extent the orthosis can be reheated and refolded to allow a cost-effective implementation of the orthosis from the start.

Furthermore, the orthosis has to be tested on more volunteers to optimize the algorithm and to test wear comfort of modifications. The thickness of the ORFIT sheets could be increased from 3.2 to 4.2mm to increase strength with (a theoretical) 39% if the orthosis does not provide sufficient support for clinical applications after improving the closing mechanism.

9 CONCLUSION

The goal of this thesis was to develop a method to quickly manufacture an orthosis for distal radius fractures. Different options were considered but eventually, it was decided to produce the orthosis by laser cutting out of a thermoformable plastic material which is then to be folded around the arm. With this method, finish smoothness and speed can be combined with relatively low cost.

In this stage of the process, many manual operations are necessary to produce the 2D or 3D design of the orthosis. However, during the development of the product, more steps became automatic and when a higher volume is necessary, automation can be realised without too much effort.

With the objective of increasing production speed, thermoforming in combination with laser cutting has achieved its goal, it is significantly faster than 3D printing. It does come at a few costs. More skill is required of the people applying the orthosis compared to 3D printing the orthosis but is similar to conventional casts. Folding from 2D to 3D always causes a few distortions that cannot be taken into the design due to limitations of using one sheet without cuts.

Thermoforming combined with laser cutting can boost implementation speed by being sufficiently fast to be implemented at this moment in time. When 3D printing with high-quality finishes becomes quicker and less expensive, it may have more benefits. However, this may take years and right now orthosis can be produced quickly and with relatively low cost by combining the right thermoformable material with laser cutting technology.

10 REFERENCES

1. Nellans KW, Kowalski E, Chung KC. The Epidemiology of Distal Radius Fractures. *Hand Clin*. 2012;28(2):113-125. doi:10.1016/j.hcl.2012.02.001
2. Stirling ERB, Johnson NA, Dias JJ. Epidemiology of distal radius fractures in a geographically defined adult population. *J Hand Surg (European Vol*. 2018;43(9):974-982. doi:10.1177/1753193418786378
3. Chen Y-J, Lin H, Zhang X, Huang W, Shi L, Wang D. Application of 3D–printed and patient-specific cast for the treatment of distal radius fractures: initial experience. *3D Print Med*. 2017;3(1):11. doi:10.1186/s41205-017-0019-y
4. Inglis M, McClelland B, Sutherland LM, Cundy PJ. Synthetic versus plaster of Paris casts in the treatment of fractures of the forearm in children. *Bone Joint J*. 2013;95-B(9):1285-1289. doi:10.1302/0301-620X.95B9.30666
5. Halanski M, Noonan KJ. Cast and Splint Immobilization: Complications. *J Am Acad Orthop Surg*. 2008;16(1):30-40. doi:10.5435/00124635-200801000-00005
6. Xkelet. https://www.xkelet.com/en/. Accessed November 19, 2019.
7. ActivArmor. https://activarmor.com/. Accessed November 19, 2019.
8. Cortex. https://www.evilldesign.com/cortex. Accessed November 19, 2019.
9. Castprint. http://castprint.co/cast-solutions/. Accessed November 19, 2019.
10. Anusci V. ActivArmor May Have Finally Cracked the 3D Printed Cast/Orthosis Riddle. 3D printing media network. https://www.3dprintingmedia.network/activarmor-may-finally-cracked-3d-printed-cast-orthosis-riddle/. Published 2018. Accessed October 16, 2019.
11. Delft EAK van, Gelder TG van, Vries R de, Vermeulen J, Bloemers FW. Duration of Cast Immobilization in Distal Radial Fractures: A Systematic Review. *J Wrist Surg*. 2019;08(05):430-438. doi:10.1055/s-0039-1683433
12. Fixit. https://usefix.it/. Accessed November 21, 2019.
13. Finished PFOR, Properties A. Rolyan ® Splinting Materials. 1993.
14. Silva MJ, Gibson LJ. The effects of non-periodic microstructure and defects on the compressive strength of two-dimensional cellular solids. *Int J Mech Sci*. 1997;39(5):549-563. doi:10.1016/S0020-7403(96)00065-3
15. Angelucci G, Mollaioli F. Voronoi-Like Grid Systems for Tall Buildings. *Front Built Environ*. 2018;4(December):1-20. doi:10.3389/fbuil.2018.00078
16. Fazekas A, Dendievel R, Salvo L, Bréchet Y. Effect of microstructural topology upon the stiffness and strength of 2D cellular structures. *Int J Mech Sci*. 2002;44(10):2047-2066. doi:10.1016/S0020-7403(02)00171-6
17. Lafontaine M, Hardy D, Delince P. Stability assessment of distal radius fractures. *Injury*. 1989;20(4):208-210. doi:10.1016/0020-1383(89)90113-7
18. Walenkamp M, Vos L, Strackee S, Goslings J, Schep N. The Unstable Distal Radius Fracture—How Do We Define It? A Systematic Review. *J Wrist Surg*. 2015;04(04):307-316. doi:10.1055/s-0035-1556860
19. Marsell R, Einhorn TA. The biology of fracture healing. *Injury*. 2011;42(6):551-555. doi:10.1016/j.injury.2011.03.031
20. Claes L, Recknagel S, Ignatius A. Fracture healing under healthy and inflammatory conditions. *Nat Rev Rheumatol*. 2012;8(3):133-143. doi:10.1038/nrrheum.2012.1
21. Hofman M, Koopmans G, Kobbe P, et al. Improved Fracture Healing in Patients with Concomitant Traumatic Brain Injury: Proven or Not? *Mediators Inflamm*. 2015;2015:1-14. doi:10.1155/2015/204842

22. Jensen MR, Andersen KH, Jensen CH. Management of undisplaced or minimally displaced Colles' fracture: One or three weeks of immobilization. *J Orthop Sci*. 1997;2(6):424-427. doi:10.1007/BF02488930
23. Andrushko JW, Gould LA, Farthing JP. Contralateral effects of unilateral training: sparing of muscle strength and size after immobilization. *Appl Physiol Nutr Metab*. 2018;43(11):1131-1139. doi:10.1139/apnm-2018-0073
24. Kalantari M, Nechifor M. Accuracy and utility of the Structure Sensor for collecting 3D indoor information. *Geo-Spatial Inf Sci*. 2016;19(3):202-209. doi:10.1080/10095020.2016.1235817
25. Silva M, Avoian T, Warnock RS, Sadlik G, Ebramzadeh E. It is not just comfort: waterproof casting increases physical functioning in children with minimally angulated distal radius fractures. *J Pediatr Orthop B*. 2017;26(5):417-423. doi:10.1097/BPB.0000000000000372
26. Brinke J ten. Development of a new brace design for immobilization of a distal radius fracture based on a biomechanical model for colles' type fractures. 2019.
27. Li J. Rapid customization system for 3D-printed splint using programmable modeling technique – a practical approach. *3D Print Med*. 2018. doi:10.1186/s41205-018-0027-6
28. Zhang X, Fang G, Dai C, et al. Thermal-Comfort Design of Personalized Casts. In: *Proceedings of the 30th Annual ACM Symposium on User Interface Software and Technology - UIST '17*. New York, New York, USA: ACM Press; 2017:243-254. doi:10.1145/3126594.3126600
29. (ULS) ULS. PLA. https://www.ulsinc.com/materials/pla. Accessed November 11, 2019.
30. Nieuwenhof H van den. *Stiffness of 3D Printed Orthoses for Fixation of Distal Radius Fractures; Unpublished Report (Clinical Rotation Technical Medicine, University of Twente),*. Arnhem; 2020.
31. van Wijk MWM. *Quantitative Assessment of The Stiffness of Fiberglass Forearm Casts With The Purpose of Improving Distal Radius Fracture Therapy; Unpublished Report (Clinical Rotation Technical Medicine, University of Twente)*. Arnhem; 2019.
32. Amber van Elburg, Eva Groenendijk, Koen Storck T van Z. *Advies over de Materiaaleigenschappen van Een Geprinte Orthese Bij de Alternatieve Behandeling van Stabiele, Niet-Verplaatste Colles-Fracturen, Unpublished Report (Multidisciplinary Assignment, University of Twente)*. Enschede; 2018.
33. Mihalko WM, Beaudoin AJ, Krause WR. Mechanical Properties and Material Characteristics of Orthopaedic Casting Material. *J Orthop Trauma*. 1989;3(1):57-63. doi:10.1097/00005131-198903010-00011
34. Pirhonen E, Pärssinen A, Pelto M. Comparative study on stiffness properties of WOODCAST and conventional casting materials. *Prosthet Orthot Int*. 2013;37(4):336-339. doi:10.1177/0309364612465885
35. Öztürk A, Çiçek B, Mazıcıoğlu MM, Zararsız G, Kurtoğlu S. Wrist Circumference and Frame Size Percentiles in 6-17-Year-Old Turkish Children and Adolescents in Kayseri. *J Clin Res Pediatr Endocrinol*. 2017;9(4):329-336. doi:10.4274/jcrpe.4265
36. Santoni BG, Aira JR, Diaz MA, Kyle Stoops T, Simon P. Radiographic evaluation of acute distal radius fracture stability: A comparative cadaveric study between a thermo-formable bracing system and traditional fiberglass casting. *Clin Biomech*. 2017;47:20-26. doi:10.1016/j.clinbiomech.2017.05.009
37. Hoogervorst P, Knox R, Tanaka K, et al. A Biomechanical Comparison of Fiberglass

Casts and 3-Dimensional-Printed, Open-Latticed, Ventilated Casts. *Hand (N Y)*. February 2019:1558944719831341. doi:10.1177/1558944719831341
38. Li J, Tanaka H. Feasibility study applying a parametric model as the design generator for 3D–printed orthosis for fracture immobilization. *3D Print Med*. 2018;4(1):1. doi:10.1186/s41205-017-0024-1

11 APPENDIX

Table A-1 measured and calculated values of the stiffness validation setup

	Load	Displacement		Degree Angle		Radial angle	
Flexion01		**Total**	**Net**	**Total**	**Net**	**Total**	**Net**
1 t/m 3	0 kg	19	-	?	n/a	n/a	n/a
Number 4	4 kg	n/a	n/a	3,5	n/a	0,061	n/a
Number 5	8 kg	n/a	n/a	4,8	n/a	0,084	n/a
Number 6	12 kg	35	16	6,4	n/a	0,112	n/a
Extension01							
Number 7	0 kg	32	0	5,7	0	0,099	0,000
Number 8	4 kg	40	8	6,4	0,7	0,112	0,012
Number 9	8 kg	44	12	11,6	5,9	0,202	0,103
Number 10	12 kg	49	17	14,8	9,1	0,258	0,159
Extension02							
Number 11	4 kg	44	-	8,3	2,6	0,145	0,045
Number 12	8 kg	49	5	11	5,3	0,192	0,093
Number 13	12 kg	54	10	12,9	7,2	0,225	0,126
Flexion02							
Number 14	0 kg	20	0	0	0	0,000	0,000
Number 15	4 kg	25	5	2,3	2,3	0,040	0,040
Number 16	8 kg	30	10	2,6	2,6	0,045	0,045
Number 17	12 kg	30*	10	3	3	0,052	0,052
*** something shifted; red = prediction**							